A yeast two-hybrid screen in *Arabidopsis thaliana* suggests FORKED1 forms homodimers and the ARFA1 family has a role in cotyledon vein patterning.

JESSICA ERICKSON

B Sc. (Honours) University of Lethbridge, Lethbridge, 2009

A Thesis Submitted to the School of Graduate Studies of the University of Lethbridge in Partial Fulfillment of the Requirements for the Degree

MASTER OF SCIENCE

Biological Sciences

University of Lethbridge

LETHBRIDGE, ALBERTA, CANADA.

This thesis is dedicated to Trent Schuler, who kindled my love for biology and introduced me to Mendel.

Abstract

The plant hormone auxin is essential for cell differentiation into vascular tissue, and leaf cells that will become veins show asymmetric distribution of the plasma membrane protein PINFORMED1 (PIN1), which directs auxin flux. The formation, sorting and transport of PIN1 vesicles within the endomembrane system leads to a higher concentration of PIN1 on one membrane face. Many proteins are involved in directing PIN1 to target membranes, including FORKED1 (FKD1). A yeast two-hybrid cDNA library screen was performed to identify protein interacters that might provide information about the molecular mechanism of FKD1. Results suggested that FKD1 is capable of forming homodimers through its DUF828 domain, but that this interaction depends on the absence of the 57 N-terminal amino acids. A second protein interacter was identified, ARFA1e, but was later found to be a false positive. Despite the lack of interaction with FKD1, *arfa1e-1* mutants displayed a subtle vascular cotyledon phenotype characterized by increased vein number and increased vein meeting. The *arfa1e-2* allele and mutants in closely related genes (*arfa1a* and *arfa1b*) displayed similar defects. Double mutants showed an increase in phenotypic severity, supporting the notion that these proteins are acting redundantly during establishment of cotyledon vein pattern.

Acknowledgements

First and foremost I would like to thank Dr. Elizabeth Schultz, who sparked my interest in developmental genetics, and who encouraged me to pursue my M Sc. You provided much-needed guidance, support, and optimism despite major setbacks during the production of this thesis.

I would also like to thank:

Lab mates – Shankar, Neema, Vanessa, Emily, Jordan – I can't thank you enough for your help. Shankar you deserve a special thank you for calming me down, making me laugh, and being unfailingly patient.

Family – Mom, Dad, Katelyn, Kelsey and Mitchel – you are always ridiculously supportive and encouraging, and I love you. Mom I am sure that you experienced as much anxiety over my thesis as I did, thank you for listening.

Friends – Ashley, Brendan, Lisa, Benji, Christine, and Sandeep – you visited me in the lab at all hours of the night, distracted me when I needed it, and I would not have made it without you.

Collaborators – Dr. Susanne Kohalmi – you have acted as a teacher, a mentor, and a friend, making my time in London unforgettable. Danielle Styranko – you taught me all the ins and outs of the yeast two-hybrid, and answered an endless stream of questions

Committee – Dr. Anthony Russell and Dr. Ute Kothe – thank you for your suggestions and encouragement throughout the last two years.

Financial support – thanks to the University of Lethbridge (teaching assistantships), NSERC (CGS M scholarship), Alberta Government (Queen Elizabeth II scholarship, Alberta Graduate Student Scholarship, Alberta Profiling Award)

Table of Contents

List of Tables

List of Figures

Abbreviations and Acronyms

Gene and Protein annotation

FKD1 – wild-type gene is capitalized and italicized

fkd1 – mutant gene is italicized

FKD1 – protein is capitalized

Growth medium annotation

Growth medium lacking a given amino acid features a minus sign prior to the abbreviated amino acid name. All other essential amino acids are present.

e.g. -leu = media lacking leucine

Genes

AR1 – ARABIDOPSIS CYTOCHROME REDUCTASE1

ARF – ADP-RIBOSYLATION FACTOR

ARF1-6 – ADP-RIBOSYLATION FACTOR1-6

ARFA1a - ARFA1e – ADP-RIBOSYLATION FACTORA1a-e (ARFA1 family)

Athb8 – ARABIDOPSIS THALIANA HOMEOBOX8

AUX – AUXIN RESISTANT1

CRC – CRUCIFERIN C

CVL1 – CVP2-LIKE1

CVP2 – COTYLEDON VASCULAR PATTERN2

ERD15 – EARLY RESPONSIVE TO DEHYDRATION15

FKD1 – FORKED1

GBF1 – GOLGI-SPECIFIC BREFALDIN A-RESISTANT GUANINE NUCLEOTIDE EXCHANGE FACTOR1

GAL1, 4, 80 – GALACTOSE1, 4, 80

GNL1 – GNOM-LIKE1

GNOM

GRP2 – GLYCINE RICH PROTEIN2

LAX1, 2, 3 – LIKE AUXIN1, 2, 3

MP – MONOPTEROS

OE23 – OXYGEN EVOLVING COMPLEX SUBUNIT23

PIN1, 3, 4, 7 – PINFORMED1, 3, 4, 7

SEN1 – SENESCENCE 1

SFC/VAN3 – SCARFACE/VASCULAR NETWORK3

UBC28 – UBIQUITIN-CONJUGATING ENZYME28

Chemicals and Solutions

3AT – 3-amino-1, 2, 4-triazole

BFA – Brefaldin A

IAA- or IAAH – indole-3-acetic acid

LiAc – lithium acetate

LB – Luria Bertani growth medium

NPA – 1-N-naphthylphthamic acid

PEG - polyethylene glycol 3350

SD – synthetic dextrose

S.O.C. – super optimal broth with catabolite repression

TE – Tris EDTA

X-gal – bromo-chloro-indolyl-galactopyranoside

Additional Abbreviations

ACAPs – ARF-GAP with coiled coil, ankyrin repeats, and a PH domain

ADP – adenosine diphosphate

ARF-GAPs – ADP-ribosylation factor GTPase activating proteins

ARF-GEFs – ADP-ribosylation factor-guanine exchange factors

BAR domain – Bin-Amphiphysin-Rvs domain

cDNA – complementary DNA

DAG – days after germination

DB – DNA binding domain

DUF828 – Domain of unknown function828

His – histidine

IAA - auxin

Leu – leucine

LTP – lipid transfer protein

MATa – mating type a

MATα – mating type α

MCS – multiple cloning site

PA – phosphatidic acid

PCR – polymerase chain reaction

PED – PIN expression domain

PH domain – Pleckstrin Homology domain

PI – phosphotidylinositol

PI(3,5)P – phosphotidylinositol 3, 5-phosphate

PI(4)P – phosphotidylinositol 4-phosphate

PI(4, 5)P_2 – phosphotidylinositol 4, 5-biphosphate

5PTase – inositol phosphate 5'-phosphatases

RT-PCR – reverse transcription-polymerase chain reaction

TA – transcription activation domain

T-DNA – transferred DNA

TGN – trans-golgi network

Trp - tryptophan

UAS_G - upstream activating sequence recognized by GAL4

UTR – untranslated region

Terms

Apical – closest to leaf tip/apex

Basal – closest to leaf base/stem

Lateral – at 90^o angles to apical and basal

Oblique – angles other than 90^o

Electronic Resources

EMBOSS needle alignment (www.ebi.ac.uk)

Predict Protein (www.predictprotein.org)

Primer Plus (www.bioinformatics.nl/cgi-bin.primer3plus.primer3plus.cgi)

TAIR (www.arabidopsis.org)

TAIR BLAST 2.2.8 (www.arabidopsis.org/Blast/index.jsp)

1. Introduction

Development of all multi-cellular organisms requires coordination between cells, each adopting a fate appropriate for its position. Thus, cells require positional information to develop into a functioning organism. During the development of all plants the polar transport of phytohormones called auxins is essential for embryo axis formation, shoot outgrowth, root development, organ initiation/positioning, vascular development, and tropic responses (Reinhardt et al., 2003; Friml et al., 2002b; Abel and Theologis, 2010). The wide range of roles filled by auxins can be explained by differences in hormone level as well as cell perception, which is largely dependent on spatial and temporal factors such as tissue type and developmental stage (Vieten et al., 2005). This thesis will focus on a role for auxin during patterning of leaf vein tissue.

1.1 Auxin canalization as a model for vein patterning

Arabidopsis thaliana is frequently used as a model for leaf vein formation in dicotyledonous plants (Nelson and Dengler, 1997). *Arabidopsis* leaves exhibit a hierarchical vein pattern, with lower order veins branching from higher order veins. Veins form a closed reticulate pattern, with lower order veins joined to higher order veins at both ends. An exception is the smallest order veins, where one end often fails to connect to the network, creating 'freely ending' veins.

Auxin induced vein formation has been suggested to rely on a positive feedback loop, where auxin up-regulates its own flux (Sachs 1981; Sachs 1991). This theory predicts that auxin should initially be widespread and uniform, but random fluctuations in concentration should lead to up-regulated flux in some cells over

others, subsequently increasing auxin movement through these cells. Preferred routes of 'auxin canalization' are established in this way. Auxin flux occurs directionally with two outcomes: 1) auxin is drained from neighboring cells into the 'canal', and 2) auxin is transported through 'canals' along its concentration gradient from high (sources) to low (sink) concentrations. In this way 'canals' become increasingly narrow, maintaining auxin levels high enough to specify the formation of vein cells (Sachs, 1989).

1.2 Auxin flux

A prerequisite for auxin canalization is auxin flux, which occurs by diffusion and by active transport. Indole-3-acetic acid (IAA) is the major source of auxin in plants and can exist in its protonated form (IAAH) or unprotonated (IAA-), of which only IAAH is capable of diffusion through the plant cellular membrane (Kramer and Bennett, 2006). The low pH of the extracellular space (~5) favors the association of IAA- with protons about 20% of the time, allowing for diffusion through the plasma membrane, while the neutral pH inside cells favors anionic auxin (Kramer and Bennett, 2006). Diffusion of only 20% of auxin is not sufficient to entirely account for rapid and directional auxin fluxes exhibited by plants (Kramer and Bennett, 2006), but auxin movement can be explained via the active transport of anionic auxin into and out of the cell by membrane bound carrier proteins (Swarup et al., 2004; Steinmann et al., 1999). The polar localization of these carrier proteins is critical to the formation of gradients through the establishment of directional auxin fluxes (Bennett et al., 1996; Steinmann et al., 1999).

In Arabidopsis four proteins have been implicated in auxin influx, AUXIN RESISTANT1 (AUX1) and LIKE AUX1, 2, 3 (LAX1-3) (Bainbridge et al., 2008). These proteins are members of an amino acid/auxin permease family, and act as proton-driven symporters to facilitate the influx of IAA- and H+ simultaneously (Swarup et al., 2004; Bennett et al., 1996). *LAX* amino acid sequences are 73-83% similar to *AUX1*, and a mutation in any one of these four genes induces defects in auxin regulated processes (Swarup et al., 2004; Parry et al., 2001). Defects are presumably due to the inability of mutants to create sharp and dynamic auxin maxima. This concept is demonstrated in the shoot apical meristem of *aux1 lax1 lax2* triple mutants, which exhibit weak and broad expression of the auxin response reporter *DR5:GUS* relative to wild type (Bainbridge et al., 2008). Aberrant expression and distribution of *DR5:GUS* is correlated with formation of fewer leaves, irregular phylotactic patterns, and arrest of organ formation (Bainbridge et al., 2008), highlighting the importance of auxin influx to leaf formation.

Auxin efflux is largely facilitated by PIN family proteins, of which PIN1, 3, 4 and 7 show the most polar localization during embryo development, organ development, and tropic responses (Zazimalova et al., 2010). PINs are imperative to directional auxin efflux, and as a result are involved in a wide variety of developmental processes. PIN1 acts in vascular development and organ initiation/positioning (Reinhardt et al., 2003); PIN3 facilitates differential cell elongation during shoot outgrowth, and tropic responses, such as downward root growth in response to gravity, or shoot turning towards light (Friml et al., 2002b); PIN4 acts to maintain stem cells of the root apical meristem (Friml et al., 2002a);

PIN7 is involved in defining embryo polarity through the establishment of an apical-basal auxin gradient (Friml et al., 2003). Although there appears to be functional division of labor between the family members to maintain auxin fluxes in different tissue types, loss of function mutations in one *PIN* can be compensated for by the ectopic expression of other family members (Vieten et al., 2005), indicating functional redundancy. This is supported by the subtle phenotypes of the *PIN* single mutants and double mutants compared to *pin 1, 3, 4,* 7, quadruple mutants, which exhibit increased embryonic defects, and are often lethal (Vieten et al., 2005). Chemical inhibition of auxin efflux with 1-N-naphthylphthamic acid (NPA) also leads to severe embryonic defects, sometimes resulting in ball-shaped embryos lacking apical and basal polarity specification or embryos with cup shaped cotyledons (Friml et al., 2003).

Transcription profiling reveals that *PIN1*, *3*, *4*, and *7* are expressed globally during the development of the plant, but exhibit tissue specific variations in expression level and polar localization (Vieten et al., 2005). However, in the leaf primordia *PIN1* is the only family member expressed in the early ground meristem prior to the procambial marker *Athb8*, which predicts the development of vascular tissue (Scarpella et al., 2006). Emphasizing its importance in vein patterning, *pin1* leaves exhibit vascular defects such as increased marginal vasculature and number of central vascular strands (Mattsson et al., 1999). The unique role of PIN1 in the differentiation of veins provides an opportunity to isolate the effect of a single PIN on auxin flux and the resultant vascular phenotype.

1.3 PIN1 involvement in auxin canalization

The 'canalization' model of vein formation predicts the directional transport of auxin along preferred routes, draining surrounding cells and triggering cell specification. Despite the proposal of the 'auxin canalization' hypothesis prior to the discovery of efflux proteins, the model predicts PIN1 expression patterns accurately. PIN1 expression domains (PEDs), monitored by fusion of PIN1 to green fluorescence protein (PIN:GFP), form continuous closed loops representative of the final vein pattern (Scarpella et al., 2006). PEDs are initially wide, overlapping with broad fields of auxin, and narrow as preferred routes of auxin are established, supporting the idea that auxin regulates its own flux through *PIN1* (Scarpella et al., 2006; Hou et al., 2010; Wenzel et al., 2007). Consistent with this idea, application of exogenous auxin increases global levels of *PIN1* transcript (Vieten et al., 2005), as well as increasing initial size of PIN1 expression domains in young leaf primordia (Scarpella et al., 2006). PED narrowing is delayed in leaf primordia treated with low levels of NPA and the phenotype mimics that of *pin1*, providing evidence for the interdependence of auxin flux and PIN1 narrowing (Scarpella et al., 2006). The influence of auxin on *PIN1* expression may be through induction of the transcription factor MONOPTEROS (MP), which activates transcription of other auxin inducible genes (Wenzel et al., 2007). In the absence of *MP* expression PIN1:GFP expression is reduced, and auxin inducible PIN1 transcription is abolished, indicating MP may activate transcription of PIN1 as part of the positive feed-back loop (Veiten et al., 2005; Wenzel et al., 2007).

The 'auxin canalization' model also predicts localization of PIN1 away from auxin 'sources' and towards auxin 'sinks'. High auxin concentrations in cells at the leaf tip are suggested to drive transition of PIN1:GFP localization from membranes facing the leaf tip (Figure 1A), to oblique, lateral and basal localization (Figure 1B), theoretically directing auxin away from maxima (source) and into subepidermal cell layers (sink) where the midvein forms (Bayer et al., 2009). Oblique localization is gradually reduced and PIN1:GFP exhibits only two polarities in the incipient midvein; 1) basal localization away from the convergence point, suggesting auxin flux through the incipient midvein towards the stem, and 2) lateral localization, presumably draining auxin from surrounding cells into the midvein (Figure 1C) (Bayer et al., 2009; Scarpella et al., 2006). PIN1:GFP localization patterns are similar during initiation of vein loops. PIN1:GFP is localized away from auxin convergence points, or 'sources', and drained into previously formed vascular tissue, which would acts as 'sinks' (Scarpella et al., 2006). Formation of a closed loop requires the meeting of two PIN1 expression domains, both of which transport auxin to previously formed vascular tissue but in opposite directions (Scarpella et al., 2006). Opposing auxin fluxes are joined by the bipolar cell, which exhibits PIN1:GFP localization on two opposite membranes, and is thus predicted to transport auxin in both directions (Scarpella et al, 2006; Hou et al., 2010; Wenzel et al., 2007).

1.4 Clathrin mediated vesicle formation

The flexible and rapid alterations in PIN1 distribution patterns exemplified during the formation of the midvein and vein loops is hypothesized to occur through cycling of PIN1 between the plasma membrane and endosomes by transport

vesicles (Dhonukshe et al., 2007). In eukaryotes, clathrin mediated vesicle formation is central for regulating the abundance of transmembrane proteins such as PINs, at both the cellular membrane, and the intracellular membranes of the Trans-Golgi Network (TGN) (Kitakura et al., 2011; Schmid, 1997; Perez-Gomez and Moore, 2007). Formation of a transport vesicle involves invagination of the donor membrane, resulting in the formation of a 'pit-like' structure, which is then pinched from the membrane (Schmid, 1997). Cytosolic clathrin proteins are recruited to the site of vesicle formation where they assist in deforming the membrane and the recruitment of cargo proteins (Schmid, 1997). The formation of a completed transport vesicle is achieved by GTPase mediated constriction and excision to form a mobile, circular membrane fragment (Schmid, 1997). Prior to vesicle fusion with a target membrane the clathrin coat must dissociate (Schmid, 1997).

In *Arabidopsis* root cells, clathrin partially co-localizes with PIN proteins suggesting a role for clathrin in the formation of PIN1 vesicles (Dhonukshe et al., 2007). Endocytosis of PIN1 is inhibited in protoplasts when clathrin lattice formation is inhibited, in clathrin mutants, and following the induction of dominant negative clathrin (Dhonukshe et al., 2007; Kitakura et al., 2011), indicating that endocytosis of PIN1 is dependent on clathrin (Dhonukshe et al., 2007). Subsets of clathrin mutants resemble auxin transport mutants in both phenotype and auxin distribution, correlated with apolar distribution of PIN1 in root cells (Kitakura et al., 2011). Thus, clathrin mediated endocytosis of PIN1 is required for PIN1 polarity, and hence for auxin transport (Kitakura et al., 2011).

The requirement for PIN1 endocytosis prior to polar distribution suggests that at least some PIN1 proteins are being re-cycled between the cell membrane and endosomes, and re-distribution is not solely the result of de-novo protein synthesis. Evidence for the re-cycling of PIN1 is provided when roots are treated with the protein synthesis inhibitor cycloheximide for 4 hours and there is no decrease in PIN1 at the cell membrane, suggesting protein synthesis is not required for polarity, and that PIN1 turnover is slow (Geldner et al., 2001).

1.5 ADP-ribosylation factors

ADP-ribosylation factors (ARFs) were first identified in mammals as cofactors in the activation of adenylate cyclase, an enzyme important for the production of important second messenger cAMP (Szopa and Sikorski, 1994). Later it was discovered that ARFs were GTPases involved in the recruitment of clathrin coat during the formation of a vesicle (Bonifacino and Jackson, 2003). ARFs have been subdivided into classes I, II, and III based on sequence similarity (Jackson and Casanova, 2000). Class I ARFs are most well characterized and have a known role in vesicle formation at the golgi, the TGN, and endosomal membranes. Class I ARFs include human ARFs 1-3, yeast ARFs 1 and 2, and *Arabidopsis* ARFs 1-6 (Jackson and Casanova, 2000; Bonafacino and Jackson, 2003; Gebbie et al., 2005). They show high sequence similarity between all organisms, and one representative in *Arabidopsis, ARFA1c* rescues yeast with *arf1*/*arf 2* mutations, which are typically fatal (Gebbie et al., 2005). Very little is known about the other two ARF classes. Class II ARFs include mammalian ARFs 4 and 5, and class III includes only mammalian ARF 6 (Jackson and Casanova et al., 2000). In mammals ARF6 has been implicated in endocytosis

and membrane recycling, and is localized to both the plasma membrane and endosomes (Jackson et al., 2000).

During vesicle cycling, ARFs cycle through GTP and GDP bound forms (Figure 2). GTP bound ARFs form a stable association with donor membranes through hydrophobic residues at the N-terminus (Jackson and Casanova, 2000). ARF-GTP sorts trans-membrane cargoes and recruits coat proteins necessary for vesicle budding (Gebbie et al., 2005). Following budding of the vesicle, ARF-GTP undergoes hydrolysis and a conformation change concealing the hydrophobic residues, and thus destabilizes the interaction with the membrane (Jackson and Casanova, 2000). Cytosolic ARF-GDP triggers coat dissociation, which must occur prior to docking and fusion of vesicles with target membranes (Jackson and Casanova, 2000). Nucleotide exchange rate is slow when ARFs act alone. Exchange rate is augmented by ADP ribosylation factor – guanine nucleotide exchange factors (ARF-GEFs) to form ARF-GTP, and by ADP-ribosylation factor GTPase activating proteins (ARF-GAPs) (Figure 2), which increase the rate of hydrolysis to form ARF-GDP (Scheffzek et al., 1998).

1.6 ARF-GEFS in Arabidopsis

Considerable evidence suggests that an *Arabidopsis* ARF-GEF, GNOM, plays a role in the cycling of PIN1 from the endosome (Naramoto et al., 2010; Richter et al., 2007). *gnom* mutants phenocopy quadruple mutant phenotypes of *pin1, 3, 4, 7* embryos (Geldner et al., 2003). Mutant alleles may result in lack of embryonic apical basal polarity, roots, hypocotyls, cotyledons, and occasionally display organ fusions (Geldner et al., 2003). Less severe *gnom* alleles, such as *emb30-7*, have an altered vascular phenotype with excess elements along the leaf margin and enlarged veins

reminiscent of *pin1* single mutant vasculature (Koizumi et al., 2000). Both severe and mild *gnom* phenotypes can be mimicked by treatment with high or low NPA respectively (Mattsson et al., 1999; Geldner et al., 2003), suggesting that the *gnom* phenotype is the result of a defect in auxin efflux. In congruence with this theory, PIN1 shows random polar localization and general lack of organization in *gnom* (Steinmann et al., 1999), suggesting that GNOM is essential for targeting of PINs to the appropriate cell membrane.

GNOM is one of five *Arabidopsis* ARF-GEFS inhibited by the fungal toxin Brefaldin A (BFA). BFA acts by binding to hydrophobic residues of the Sec7 domain of the ARF-GEF protein. This binding stabilizes the association of ARF-GDP with the ARF-GEF at the donor membrane, thus preventing conversion to ARF-GTP (Jackson and Casanova, 2000; Richter et al., 2007). BFA treatment of *Arabidopsis* roots induces the formation of two large intracellular compartments formed through the aggregation of vesicles derived from the golgi stacks and endosomal compartments of the trans-golgi (Geldner et al., 2001). Treatment with BFA for 30 minutes results in accumulation of internal PIN1 at aggregate membranes and the elimination of polar PIN1 localization (Geldner et al., 2001; Steinmann et al., 1999). A mutation in the Sec7 domain of *GNOM* that renders it BFA resistant is also sufficient for restoring proper PIN1 localization in the presence of the toxin (Richter et al., 2007). This supports the idea that GNOM is the only BFA sensitive ARF-GEF essential for budding of PIN1 filled vesicles bound for the plasma membrane.

Continued intracellular accumulation of PIN1 in weak *gnom* alleles (Naramoto et al., 2010) and during BFA treatment (Steinmann et al., 1999) suggests

that GNOM is not uniquely required for vesicle budding during endocytosis, and that resistant ARF-GEFs could play a role (Richter et al., 2007). Mutants in *GNOM-LIKE1* (*GNL1*), a BFA resistant *GNOM* homolog with a known role vesicle cycling between the ER and golgi (Richter et al., 2007), show defects in PIN internalization following treatment with BFA (Naramoto et al., 2010). Further, plants with a GNL1, rendered sensitive to BFA, in combination with the sensitive GNOM, showed a reduction in PIN1 internalization when treated with BFA (Richter et al., 2007; Naramoto et al., 2010). Together, these results indicate that GNL1 may contribute to PIN recycling from the plasma membrane through a role in endocytosis.

Other ARF-GEFs are likely involved in PIN1 cycling. Differences in the internalization of basal and apical PIN1 proteins following prolonged BFA treatment provide support for this idea. Basal PIN1 is totally internalized, while apical PIN1 maintains a presence internally and at the cellular membrane (Kleine-Vehn et al., 2008). Prolonged BFA treatment increases redistribution of internalized PIN1 to apical membranes, and this trend was also observed in the root tissue of weak *gnom* alleles (Kleine-Vehn et al., 2008). Continued apical localization in the absence of GNOM function suggests that BFA resistant ARF-GEFs are involved in apical PIN1 cycling (Klein-Vehn et al., 2008). Treatment with BFA during embryogenesis and during organogenesis revealed that PINs failed to basally localize, further supporting the idea that GNOM is mostly responsible for recycling leading to basal localization.

Localization of GNOM was initially only observed at the endosomal membrane (Bonifacino and Jackson, 2003), despite a suggested role in endocytosis

(Naramoto et al., 2010). This could be the result of the rapid dissociation of GNOM from the membrane and the ARF substrate following nucleotide exchange (Naramoto et al., 2010), as is the case with the human GBF1 (Szul et al., 2005). This brief interaction is independent of vesicle coat recruitment by ARF1-GTP and nucleotide exchanges triggers the release of the ARF-GEF (Szul et al., 2005). This model supports the idea that one ARF-GEF activates a single ARF before dissociation, as opposed to remaining membrane bound and activating multiple ARFs (Szul et al., 2005). The decreased mobility of sensitive ARF-GEFs following BFA treatment was exploited by Naramoto et al. (2010) to chemically "freeze" GNOM-GFP where it binds and activates its ARF targets. Even at BFA levels too low to produce "BFA compartments" there was a strong GNOM-GFP signal at the plasma membrane (Naramoto et al., 2010), indicating GNOM acts at the plasma membranes as well as being localized to the endosome.

1.7 SCARFACE/VASCULAR NETWORK3

As opposed to ARF-GEFs, which facilitate the association of ARFs with GTP, ARF-GAPs activate ARF hydrolysis of GTP (Figure 2), triggering vesicle coat dissociation and allowing for fusion with target membranes (Gebbie et al., 2005). The ARF-GAP domain binds specifically to an ARF substrate to activate its GTPase activity, allowing for vesicle coat dissociation (Goldberg 1999; Naramoto et al., 2009). Given that an ARF is capable of recruiting several different coat proteins, in multiple locations, the specific function and localization of a given ARF is likely conferred through an interaction with a specific ARF-GAP domain (Naramoto et al., 2009). SCARFACE/VASCULAR NETWORK3 (SFC/VAN3), a member of the ACAP

family of ARF-GAPs, is organized into four protein domains, the Bin–Amphiphysin–Rvs (BAR), Pleckstrin Homology (PH), ARF-GAP, and two Anykrin repeats (Sieburth et al., 2006) all of which may have a role in protein-protein interaction or membrane docking (Koizumi et al. 2005; Sieburth et al., 2006; Peter et al., 2004; Naramoto et al., 2009), consistent with the notion that the ARF-GAP directs localization of the ARF.

Mutants in *SFC*/*VAN3* exhibit a discontinuous vein phenotype, characterized by many vascular islands (Deyholos et al., 2000; Koizumi et al., 2005). Vascular discontinuity in *sfc*/*van3* mutants is strongly correlated with the inability to maintain continuous PIN1 expression (Scarpella et al., 2006). In addition to SFC/VAN3 there are three other ACAPs in *Arabidopsis*, and although only *sfc* exhibited a single mutant vein phenotype, quadruple mutants showed enhanced vascular defects compared to *sfc-9* single mutants (Jackson et al., 2000). This indicates that SFC/VAN3 is the only ACAP ARF-GAP essential to vascular continuity through an influence on PIN1, but other family members may play a minor role.

SFC/VAN3 co-localizes with TGN markers and unidentified organelles, but this localization becomes nuclear and cytoplasmic in the absence of either the BAR or PH domains (Naramoto et al., 2009). As in other organisms, the PH domain contributes to protein localization through an interaction with phosphoinositides (Naramoto et al., 2009). Phosphoinositides have a wide range of functions and are soluble or membrane bound depending on their isomeric state, which is modified by enzymes (Carland and Nelson, 2009). *In vitro* the PH domain of SFC/VAN3 shows the highest affinity for phosphotidylinositol 4-phosphate (PI(4)P), as well as weak

binding to phosphotidylinositol 4, 5-biphosphate (PI(4, 5)P_2) , and phosphotidylinositol (PI) (Koizumi et al, 2005). Binding to PI(4)P stimulated ARF-GAP activity to the greatest extent, followed by weak activation by PI(4, 5)P_2 and phosphatidic acid (PA), indicating that the affinity of the PH domain for specific phospholipid signals is important for activity as well as localization (Naramoto et al., 2009). In support of this idea ARF-GAP activity of SFC/VAN3 was eliminated in the absence of the PH domain, even in the presence of PI(4)P (Naramoto et al., 2009).

1.8 Inositol phosphate 5'- phosphatases

The importance of phosphoinositides as membrane targets of SFC is supported by mutations in inositol phosphate 5' – phosphatases (5PTases), *COTYLEDON VASCULAR PATTERN2* (*CVP2*) and *CVP2-LIKE1* (*CVL1*). These two inositol phosphate 5'-phosphatases (5PTase) utilize PI(4, 5)P_2 as a substrate to produce PI(4)P (Figure 2), which strongly stimulates SFC/VAN3 ARF-GAP activity (Carland and Nelson, 2009; Berdy et al., 2001). Double mutants *cvp2 cvl1* are a phenocopy of *sfc*/*van3*, exhibiting a disjointed vascular pattern, and an inability to maintain PIN1 expression domains and cell polarity (Naramoto et al., 2009; Carland and Nelson, 2009). These results suggest that the two 5PTases act redundantly and in the same pathway as SFC/VAN3, likely through production of phospholipids important to SFC/VAN3 localization and function (Figure 2; Naramoto et al., 2009; Carland and Nelson, 2009). SFC/VAN3 is abnormally localized to the cytoplasm in *cvp2 cvl1* double mutants, exhibiting the same localization pattern as SFC/VAN3 harboring a PH domain mutation (Naramoto et al., 2009). This supports the

hypothesis that CVP2 and CVL1 contribute to wild type SFC localization through the PH domain (Carland and Nelson, 2009; Naramoto et al., 2009). In addition, the *sfc* phenotype was similar to *van3 cvp2* double mutants, as well as *cvp2 cvl1 sfc* triple mutants (Carland and Nelson, 2009; Naramoto et al., 2009), providing further evidence that SFC/VAN3 is acting in the same pathway as CVP2.

1.9 SFC/VAN3 vs. GNOM

GNOM and SFC/VAN3 both localize to the plasma membrane and the TGN (Bonifacino and Jackson, 2003; Naramoto et al., 2009). Although they fail to overlap intracellularly, 40% of SFC/VAN3 foci overlap with GNOM foci at the cell periphery (Naramoto et al., 2010). In the root, *sfc*/*van3 gnom* double mutants demonstrate slower uptake of the endocytic marker FM4-64, and show reduced PIN:GFP internalization compared to wild type when treated with BFA (Naramoto et al., 2010). Common sub-cellular localization to the cellular membrane, as well as a reduced endocytosis in mutants, indicates that both SFC and GNOM have a role in the internalization of PIN1 (Naramoto et al., 2010). Failure to co-localize the majority of the time also indicates that these proteins are frequently acting on ARFs in distinct cell compartments (Naramoto et al., 2010).

The ARF substrates utilized by GNOM and SFC/VAN3 have not yet been identified, so it is not known whether these two proteins act on the same or different ARFs during vesicle cycling. Mutual suppression of *SFC*/*VAN3* and *GNOM* mutant allele phenotypes suggests that these proteins are acting in opposition to one another (Koizumi et al., 2005; Sieburth et al., 2006). These two proteins could be acting on the same ARF substrate, with GNOM facilitating ARF-GTP formation,

and SFC aiding hydrolysis to produce ARF-GDP (Figure 2). GNOM is hypothesized to act on class I ARFs in a similar manner to other member of the Gea/GBF subfamily of ARF-GEFs (Trang and Bui et al., 2009). If SFC/VAN3 utilizes the same substrate as previously characterized mammalian ACAP family proteins, it is likely involved in the activation of the class III ARF6 (Jackson et al., 2000). ARF6 lacks a close homolog in plants, meaning there is no obvious ARF target suggested for SFC/VAN3 (Koizumi et al., 2005). Furthermore, there are a few fundamental differences between SFC/VAN3 and other ACAPs. SFC/VAN3 binds to PI(4)P as a preferred substrate to stimulate ARF-GAP activity, whereas animal ACAPs utilize PI(3,5)P and PI(4,5)P_2 (Koizumi et al., 2005). Due to these differences it is conceivable that SFC/VAN3 could utilize class I ARFs as opposed to the class III ARF utilized in mammals. It is known that SFC/VAN3 is capable of acting on yeast ARF1 to stimulate hydrolysis (Koizumi et al., 2005).

1.10 FORKED1

Mutants in *FORKED1* (*FKD1*) have a non-meeting vascular phenotype similar to *sfc/van3* and *cvp2 cvl1* mutants. Veins of *fkd1* mutants frequently fail to form distal vein junctions near the leaf margin (Steynen and Schultz, 2003). *sfc/van3 fkd1* double mutants have a phenotype that is more severe than either single mutant, suggesting functional redundancy (Steynen and Schultz, 2003). SFC/VAN3 forms a complex with FKD1 in yeast two-hybrid and split YFP assays, and the complex is localized to the TGN (Figure 2; Naramoto et al., 2010). *FKD1* encodes a putative PH domain (Figure 3, Predict Protein, www.predictprotein.org/) that is 24% similar to that of *SFC*/*VAN3* (EMBOSS needle alignment, www.ebi.ac.uk). Following a mutation

to the PH domain of *SFC*/*VAN3*, wild type localization to the TGN is maintained, but this pattern is lost in a *fkd1* mutant background where localization becomes cytoplasmic (Naramoto et al., 2009). This indicates that the FKD1 PH domain is sufficient to maintain localization of the FKD1-SFC/VAN3 complex to the TGN, and likely recruits the ARF-GAP to the membrane by binding PI(4)P (Figure 2; Naramoto et al., 2009). In addition to a putative PH domain, FKD1 sequence also predicts the presence of a Domain of Unknown Function 828 (DUF 828) (Figure 3), which has not been characterized, but the combination of this domain with the PH domain is conserved in 9 other proteins in Arabidopsis (TAIR, www.arabidopsis.org).

Distal non-meeting in f*kd1* leaves is correlated with abnormal PIN1:GFP expression and localization (Hou et al., 2010). As previously mentioned, PIN1 is expressed in a series of closed loops in wild type, which predict where vascular tissue will form (Scarpella et al., 2006). Multiple PIN1:GFP polarities are present in a single loop, and joining PEDs of different polarities requires the establishment of a bipolar cell (Scarpella et al., 2006; Hou et al., 2010). In *fkd1*, PIN1 narrowing is delayed relative to wild type, and apical PIN1 localization and the bipolar cell are absent in 90% of *fkd1* secondary veins (Hou et al., 2010). Abnormal PIN1 localization and expression in *fkd1* suggests that the lack of vein meeting is most probably due to defective auxin canalization (Hou et al., 2010).

The *FKD1:GUS* reporter gene is expressed throughout the vasculature of the developing leaf, floral organs, root precursors, the mature root, and the stem (Hou et al., 2010). Like PIN1:GFP, expression of *FKD1:GUS* forms a closed loop pattern and FKD1 expression domains are initially wide, and then gradually narrow to a single

cell file (Hou et al., 2010). This indicates that *FKD1* is likely subject to changes in expression resulting from auxin canalization in a manner similar to PIN1 (Hou et al., 2010). In support of this hypothesis, the *FKD1* promoter contains three auxin response elements, and transcription of the gene is altered following shifts in auxin maxima induced by treatment with exogenous auxin, NPA or mutations in auxin transport genes (Hou et al., 2010). FKD1 expression is low in the proximal lamina, where auxin levels are low, and the leaf margin where auxin is highest (Hou et al., 2010). This suggests that FKD1 expression is tightly controlled by a lower limit for activation, and an upper limit inducing repression (Hou et al., 2010). FKD1 regulation by auxin, and regulation of auxin transport through PIN1 regulation suggests its participation in the positive feedback mechanism referred to in the 'auxin canalization' hypothesis.

The molecular mechanism through which FKD1 influences PIN1 has not yet been fully elucidated, but interaction with SFC/VAN3 provides some insight (Figure 2). SFC/VAN3 allows for docking, or fusion of vesicles to target membranes by triggering the dissociation of the vesicle coat. FKD1 interaction with this ARF-GAP, and co-localization to the TGN, indicates that it could facilitate fusion of PIN1 transport vesicles to membranes of the TGN, which is a central site for sorting and re-distribution of proteins internalized as part of the endocytic pathway (Gu et al., 2001). Proteins involved in the processes of recognition, docking and fusion of vesicles with target membranes frequently act as part of a larger protein complex (Xiao et al., 2001). An interaction with SFC suggests that FKD1 may be capable of forming such complexes. Further, the PH domain of either SFC or FKD1 is sufficient

for targeting this complex to specific membranes via phosphoinositide recognition (Naramoto et al., 2009), which implies that the SFC-FKD1 interaction does not involve the PH domain. Thus we speculate that the DUF828 is involved in protein-protein interaction. The identification of other complex members could provide information about the molecular mechanism of FKD1, or could identify new proteins involved in vesicle cycling of vein patterning in general. To test this hypothesis a yeast two-hybrid cDNA library was screened using FKD1 as 'bait' to identify putative protein partners.

2. Materials and Methods

2.1 Yeast two-hybrid

A yeast two-hybrid system employing the yeast GAL4 DNA binding domain (DB) as 'bait' to screen a 'prey' cDNA library fused to the GAL4 transcription activation domain (TA) for potential interactions. An interaction between 'bait' and a 'prey' protein reconstitutes GAL4 to activate transcription of two different reporter genes; *HIS3* and *lacZ* (Figure 4A). Transcription of the *HIS3* reporter allows growth on histidine free media as well as conferring resistance to the toxic histidine biosynthesis inhibitor 3-amino-1, 2, 4-triazole (3AT), whereas a lack of interaction between proteins bars cell growth (Figure 4B) (Kohalmi et al., 1997; 1998). Activation of the *E. coli lacZ* reporter gene fusion produces β-galactosidase that cleaves bromo-chloro-indolyl-galactopyranoside (X-gal) substrate to produce a blue colony (Figure 4B) (Kohalmi et al., 1998). Activation of both *HIS3* and *LacZ* reporter genes is required for cells to be considered positive for an interaction.

2.1.1 Fusion Expression Plasmids

The yeast - *E. coli* shuttle vector PBI-770 was used to clone fusion constructs in *E. coli* and express the fusion proteins in yeast, while PBI-771 was used for 'prey' fusions (Figure 5, vectors provided by Dr. Kohalmi). The multiple cloning site (MCS) used is located downstream of both the GAL4 DB of PBI-770, and the GAL4 TA of PBI-771, resulting in C-terminal fusion proteins to GAL4 domains. Plasmids carry ampicillin resistance for selection in *E. coli*, and amino acid prototrophic markers LEU2 in PBI-770, and TRP1 in PBI-771 for selection in yeast (Kohalmi et al., 1997). Plasmids were maintained in *E. coli* and yeast during cell replication via the

inclusion of the PMB1 and CEN6/ARSH4 origins respectively, both of which tightly controlled copy in both organisms (Kohalmi et al., 1998). A yeast alcohol dehydrogenase promoter (P-ADC1) resulted in constitutive expression of both fusion proteins (Kohalmi et al., 1997). N-terminal nuclear localization signals ensured that both the 'bait' and 'prey' fusion proteins are localized to the nucleus (Kohalmi et al., 1997).

2.1.2 'Bait' vector construction

Three different GAL4 DB 'bait' fusion proteins were generated for use in the yeast two-hybrid; one with the full length FKD1 (amino acids 1-498), one with the N-terminal region (amino acids 1-221), and one with the C-terminal region (amino acids 246-498) (Figure 3). They were amplified via PCR using Phusion polymerase (New England Biolabs Inc., Pickering, ON) from the FKD1 cDNA U16276 (Arabidopsis Biological Resource Center - ABRC, Ohio State University, Columbus, OH, USA), using primers with intrinsic 5' *SALI* and 3' *NOTI* cut sites (Integrated DNA Technologies, Coralville, IA, USA) (Table 1). To allow a C-terminal fusion into the 'bait' vector relative to the GAL4 DB, primers were designed to maintain the frame of FKD1 with that of GAL4 DB and to include a stop codon (Table 1). Reverse primers for the full length FKD1 and the FKD1 C-terminal construct included the natural stop codon, while that for the N-terminal required the addition of a synthetic codon (Table 1). Amplified regions were 1500bp, 680bp, and 786bp in length for the full FKD1, the N-terminal, and the C-terminal respectively (Table 1). The PCR product was gel purified (kit from Bio Basic Inc., Markham, ON) and blunt end ligated into the pJET1.21/blunt cloning vector using the Clone Jet PCR Cloning Kit

(Fermentas, Burlington, ON). The construct was transformed into *E. coli* and plated on Luria Bertani (LB) growth medium supplemented with 50 μM ampicillin, and grown overnight at 37°C to select for colonies with the vector. DNA was extracted from *E. coli* using a commercial mini-prep kit (Bio Basic Inc., Markham, ON), digested with *SALI* and *NOTI* (New England Biolabs Inc.) and gel purified for insertion into the 'bait' plasmid, which was similarly digested and purified. *FKD1* constructs were ligated into PBI-770 using T4 DNA ligase (New England Biolabs), and transformed into *E. coli.* Transformants were grown at 37°C on selective LB + 50 μM ampicillin and DNA preparations of individual colonies were double digested with *SALI* and *NOTI* as a diagnostic test to confirm that the correct size insertion was present. Preps with a digest pattern indicating the correct insert size were sent for sequencing using primers flanking the MCS of PBI-770 (Table 2) to check that the 'bait' coding sequence was in frame with the GAL4 binding domain and lacked mutations (Nanuq, McGill University and Genome Quebec Innovation Centre, Montreal, QC).

2.1.3 'Prey' vector construction

Dr. Susanne Kohalmi generously donated the 'prey' cDNA expression library, which was made by isolating Poly [A]+ mRNA from whole *Arabidopsis thaliana* plants that were 1 to 4 weeks old (Kohalmi et al., 1997). An oligo-dT primer was used for first strand synthesis and resulting cDNAs were fragmented using *SALI* and *NOTI* enzymes for directional ligation into the MCS of PBI-771 (Kohalmi et al., 1997). This method of library construction over-represents the 3' ends of mRNAs where the primer anneals (Kohalmi et al., 1997). The cDNA library used contained

approximately 2x10^7 clones (Kohalmi et al., 1997), however only one third of these are predicted to produce a polypeptide in the same frame as the GAL4 TA.

The nature of the oligo-dT method of cDNA library construction employed leads to the formation of 'prey' fusions that feature partial cDNAs. Two protein interacters identified in library screens were chosen for confirmation experiments using the full-length 'preys': the interaction between full length FKD1 and FL13/ADP-RIBOSYLATION FACTOR A1E (ARFA1e), and the interaction between the N-terminal of FKD1 and X102/FKD1. PBI-770 and PBI-771 share the same MCS in the same frame, for a C-terminal fusion to GAL4. The three FKD1 insertions, the full-length FKD1, the N-terminal, and the C-terminal were ligated into PBI-771 from PCR products, and gel extracts made during 'bait' cloning. The process of constructing the full-length ARFA1e was identical to that of FKD1 'bait' cloning, except new primers were made for amplification of the ARF full-length cDNA U12397 (Table 1). Prey vectors were sequenced (Nanuq, McGill University and Genome Quebec Innovation Centre, Montreal, QC) to ensure they were in frame with the GAL4 TA and lacked mutations.

2.1.4 Yeast strain

YPB2 [MATa, *ura3-52*, *his3-200*, *ade2-101*, *lys2-801*, *trp1-901*, *leu2-3*, *112 canR*, *gal4-542*, *gal80-538*, *LYS1::GAL1-HIS3*, *URA3:: (GAL4$_{17mers}$)-lacZ*]

The *S. cerevisiae* strain YPB2 (provided by Dr. Susanne Kohalmi, University of Western Ontario, London, ON) was developed by Fields and Song (1989), and was used in all yeast two-hybrid screens performed. The YPB2 strain has reporter genes integrated into its genome: the *HIS3* reporter gene under *cis*-regulation of the *GAL1* upstream activating sequence (UAS_G) sequence, and the *E. coli lac*Z under the

control of the strong synthetic 17bp GAL4 UAS consensus sequence (17_{mers}) (Keegan et al., 1986). GAL4 transiently regulates reporter gene transcription following recognition of UAS_G and 17_{mers} sequences. UAS_G and 17_{mers} sequences are incorporated into the promoters of two very different genes (*LYSINE1* and *URACIL3*) so as to prevent the instance of false positives resulting from non-specific binding of the GAL4 TA construct to promoter sequences other than the GAL4 specific binding sites. A mutation in the native *GAL4* (*gal4-542*) prevents activation of reporter gene fusions in the absence of a protein interaction, while a mutation in *GAL80* (*gal80-538*) prevents repression of the GAL4 fusion protein (Kohalmi et al., 1998). To avoid the selection of revertants this strain of yeast also contains mutations in many amino acid synthesis pathways, of which *his3-200*, *lys2-801*, and *trp1-901* were used as selectable markers. The yeast cells were only of mating type (MAT a), as opposed to a mixture of MATa and MATα, in order to avoid recombination between yeast cells.

2.1.5 Yeast Media

Yeast media was made using synthetic dextrose (SD) as opposed to galactose as a carbon source, as its metabolism does not require the activation of the GAL family genes (Lohr et al., 1995), whose native regulators have been knocked out in this strain of yeast (Kohalmi et al., 1998). Media was supplemented with basic salts provided by yeast nitrogen base (without amino acids), and drop-out powder that contained adenine and uracil as well as all required amino acids except those used as selective markers. The 'bait' plasmid was selected on media that lacked leucine (-leu), 'prey' was selected on media lacking tryptophan (-trp), cells containing both

vectors were selected on media lacking both amino acids (-leu-trp) and protein interaction was selected on media lacking leucine, tryptophan and histidine (-leu-trp-his). *HIS3* is a leaky reporter gene, so basal levels of histidine are being produced at all times, thus creating histidine prototrophs that do not signify protein interaction. Due to the ability of HIS3 to confer resistance to 3AT in growth media the stringency of the HIS3 assay can be increased through elevating levels of 3AT (Kohalmi et al. 1997). This essentially requires that the cells produce more HIS3 in order to have enough resistance to overcome higher levels of 3AT in the media. The standard level of 3AT in the media is 5 mM, but may be increased to up to 25-30 mM in cases where a high stringency test is needed.

2.1.6 Lithium acetate transformation of YPB2

2.1.6.1 Preparing competent yeast cells

A high efficiency lithium acetate protocol modified from Schiestl and Gietz (1989) was used for establishing competence and transforming YPB2 cells with the PBI-770 'bait' and PBI-771 'prey' fusion constructs (protocol details in Kohalmi et al., 1998). This protocol required that cells be harvested before reaching stationary phase ($2x10^7$ cells/mL), optimally between $5x10^6$ and $8x10^6$ cells/mL. Pre-cultures were set up using 10 mL of selective SD liquid medium (Appendix) inoculated with YPB2 from a glycerol stock and incubated overnight at 30^oC. Cell density was determined using a haemacytometer and the amount of the 10mL culture required to inoculate a larger culture of –leu SD was calculated using the following formula:

$$\text{Inoculation volume} = \text{desired cell density}/\text{current cell density} \times \text{culture volume}/\ 2^{\#\ \text{of generations}}$$

Where:

desired cell density = between $5x10^6$ and $8x10^6$ cells/mL

current cell density = value calculated from the 10mL overnight culture

culture volume = usually 300mL for a ½ library screen and 700mL for a full screen

$2^{\#\ \text{of generations}}$ = this value factors in a YPB2 doubling time of approximately 2hrs and the number of generations required to reach the desired cell density

When cells reached the desired density they were centrifuged at 5000rpm for 15 minutes, washed twice with water (centrifuged at 5000rpm for 5-7 minutes and re-suspended in water 2x). Supernatant was discarded and the cells were re-suspended in LiAc solution (Appendix) to establish competence, and incubated for 1 hour at 30°C with shaking.

2.1.6.2 Transformation of competent cells

Aliquots of 200 µL and 400 µL of competent cells were used for binary screen and library screens respectively. At this stage cells can be frozen at -80°C in 100% glycerol for later use, but fresh cells were always used for library screens, as they have much higher transformation efficiency. 5 µg of transforming DNA and 20 µL of salmon sperm carrier DNA was added to competent cells, which were then incubated at 30°C for 30 minutes with shaking. 1.2 mL of PEG solution (Appendix) was then added to each tube, followed by a second incubation period of 30 minutes at 30°C with shaking. Cells were heat shocked for 15 minutes at 42°C and washed twice with 1xTE (Appendix). 200 µL of cells were then plated on appropriate selective solid SD medium and incubated at 22°C - 30°C for 3-7 days for binary screens, or at 22°C for 2-3 weeks for cDNA library screens.

2.1.7 HIS3 and X-gal Assays

To obtain sufficient cells for HIS3 and X-gal assays, transformed colonies were streaked onto appropriately supplemented SD medium; –leu for 'bait' only controls, -trp for 'prey' only controls, or –leu-trp for 'bait' and 'prey' selection. Streaks were incubated at 30°C for 3-5 days and re-suspended in 30% glycerol for storage. 10 µL of glycerol stocks were spotted onto 2 growth plates of SD supplemented for vector selection (-leu,-trp, or –leu-trp), and onto plates selective for vectors and activation of reporter genes (-leu-his+3AT, -trp-his+3AT, or -leu-trp-his+3AT). The transcription of *HIS3* was assessed after incubation for 3-7 days at 28°C by growth on the histidine free medium relative to a positive and negative control. For X-gal assays cells were lifted from growth plates with nitrocellulose filters following 2-4 days at 28°C. Filters were dipped cell side down in liquid nitrogen to lyse cells, and placed cell side up into a petri-plate containing Whatman filter paper soaked in Z-buffer (Appendix). Plates were sealed with parafilm, incubated at 28°C, and checked every half hour for β-galactosidase activity, which was assessed by the amount of blue coloration relative to the positive and negative control (Figure 4B). Interacting proteins detected in Dr. Kohalmi's lab were used as a positive control for both assays (AGL4-T4), while AGL4-T7 + an empty bait vector acted as the negative control.

2.1.8 Negative Controls

Prior to beginning cDNA library and binary screens, all 'bait' and 'prey' fusion proteins constructed were tested for the ability to activate reporter genes in the absence of protein interaction (termed self-activation). Fusion constructs were

transformed individually into YPB2 competent cells by Danielle Styranko or myself and plated on –leu to select for 'bait' only, or –trp to select for 'prey' only cells. Selected colonies were grown in streaks on appropriate selection medium and streaks were suspended in 30% glycerol stocks for HIS3 and X-gal assays. Further negative controls included the transformation of cells containing each of the 'bait' fusion constructs (full FKD1, N-terminal, or C-terminal) with an empty 'prey' vector, or a 'prey' vector containing the seed storage protein cruciferin. All cloned 'prey' constructs (full FKD1, N-terminal, C-terminal, and *ARFA1e*) were similarly tested for interaction with empty 'bait' vectors.

2.1.9 cDNA library screen

Cells that had been transformed with the full FKD1, N-terminal, and C-terminal 'bait' fusion constructs (outlined in 2.1.2) were transformed with a cDNA library via the protocol outlined in 2.1.6. 250uL of cells were plated on 145mm –leu-trp-his + 15mM 3AT selection plates and allowed to grow at room temperature for 2-3weeks. Simultaneously dilutions of 10^{-6} and 10^{-2} were plated on 82mm –leu and –leu-trp plates respectively as transformation controls. Following incubation for 2-3 days at 30^{o}C cells that grew on –leu represent those that survived the transformation protocol, and those that grew on –leu-trp represent the number of cells successfully transformed.

Following growth of transformants for 2-3 weeks at room temperature on-leu-trp-his + 15mM 3AT plates, colonies exhibiting histidine prototroph morphology (were large white or off-white, hill-like colonies, as opposed to large, white, flat colonies, or small background colonies) were streaked out and grown at 30^{o}C for 2-

3 days for glycerol stocks and were tested in a second HIS3 assay and an X-gal assay. Only yeast that could grow on –leu-trp-his + 15mM 3AT media in the second assay, and turn blue in the X-gal assay were considered positive for an interaction between the FKD1 fusion proteins and the unknown cDNA present. All others that were picked from the original screen and failed one or both assays were considered false positives.

To confirm interactions identified in the cDNA library screen the partial 'prey' cDNAs isolated from the initial screen were tested in binary assays with the full length FKD1 or the N-terminal as 'bait' in an attempt to re-create the results of the original experiment. Selected interactions identified in the library screen between FKD1 'baits' and partial 'preys' were also tested using full-length 'prey' proteins. 'Preys' constructed in 2.1.3 were transformed into cells harboring the full length FKD1 and N-terminal domain 'baits' in a yeast two-hybrid binary assay (via protocol in 2.1.6). Those colonies testing positive for both vectors were tested in HIS3 and X-gal assays as described in section 2.1.7.

2.1.10 Identification of unknown 'prey' cDNAs

2.1.10.1 Smash and grab DNA prep

DNA was extracted from yeast positive for protein interaction via a "smash and grab" prep protocol supplied by Dr. Kohalmi. Positive colonies were grown in 10mL –trp SD medium to select for PBI-771, which carried the unidentified cDNA interacter. Cells were counted using a haemacytometer and were harvested before reaching stationary phase ($2x10^7$cells/mL). Cells were centrifuged in 1.5 mL centrifuge tubes at 14,000 rpm for 2 minutes and re-suspended in 200 µL of

breaking buffer (25 phenol:24 chloroform:1 isoamyl alcohol) with acid wash beads. Cells were vortexed for two minutes, 200 μL of TE buffer pH8.0 was added, and cells were vortexed again for 10 seconds. Tubes were centrifuged for 5 minutes at 14,000 rpm and supernatant was transferred to a new tube. DNA was precipitated using 100% ethanol, spun at 14,000 rpm for 10 minutes, and pellets were washed in 70% ethanol. Pellets were allowed to air dry and were dissolved in distilled water.

2.1.10.2 Transformation into *E. coli*

For a cleaner, higher concentration preparation of the vectors, yeast DNA isolated in 2.1.10.1 was transformed into *E. coli* via electroporation. Aliquots of 20 Lμ of ElectroMAX DH5α-E cells (Invitrogen Corporation, Carlsbad, CA, USA) were transformed with 2 μL of DNA from each yeast DNA prep using the Eppendorf Electroporator 2510 (Brinkmann Instruments Inc., Mississauga, ON). Cells were thawed on ice, DNA was added, the mixture was transferred to a cuvette and electroporated at 1.7kV for 5ms. Cells were allowed to recover in 1mL Super Optimal Broth with Catabolite repression (S.O.C. Appendix) for 1 hour at 37°C with shaking at 225 rpm. Cells were then plated on LB + 50mM ampicillin.

2.1.10.3 Sequencing and identification of 'prey'

To identify the 'prey' cDNA in PBI-771 vectors the first step was to identify *E. coli* colonies that had been successfully transformed with 'prey' as opposed to FKD1 'bait'. PBI-770 and PBI-771 both carry ampicillin resistance for selection in *E. coli*. Selecting for the 'prey' plasmid using –trp selective medium only causes cells to 'kick out' approximately 30% of the 'bait' plasmids, so many cells still contain both 'bait' and 'prey' fusion constructs (Kohalmi, personal communication). This means that

35% of the *E. coli* colonies transformed with DNA isolated from yeast will likely carry the bait construct. Following electroporation (2.1.10.2) DNA preps were made from single colonies (Bio Basic Inc.) isolated on LB + 50mM ampicillin plates. Preps were digested with *SALI* and *NOTI* (New England Biolabs), as a diagnostic test to identify those that contained FKD 'bait' constructs in PBI-770, and those that contained unknown cDNA 'prey' constructs in PBI-771. Restriction patterns of preps were compared with PBI-770 + FKD1 digests, and those with alternative patterns were sent to Nanuq, McGill University and Genome Quebec Innovation Centre (Montreal, QC) for sequencing with the use of prey specific primers flanking the MCS (Table 2). TAIR BLAST 2.2.8 (TAIR, www.arabidopsis.org/Blast/index.jsp) was used to identify prey cDNAs through a sequence comparison to the *Arabidopsis thaliana* genome. The cDNA sequence data from Nanuq was also used to ensure that the prey cDNA identified was in frame with the GAL4 TA.

2.2 Phenotypic analysis of insertion mutant plants

2.2.1. Plant Growth Conditions

Seeds were planted on a mixture of ¾ potting soil (Coaldale Nurseries, Coaldale, AB) and ¼ vermiculite (Perlite Canada Inc., Montreal, QC) at a density of 15 or 25 seeds per 100cm^2 pot. Pots were then covered with plastic and incubated for 2-3 days at 4^oC, before being transferred to growth chambers (day of transfer was designated 0 DAG). Plants were grown at 22^oC under continuous light at an intensity of 130 $\mu mol \cdot sec^{-1} \cdot m^{-2}$ produced by 32W grolux and cool white Sylvania fluorescent tube lights (Osran Sylvania Inc., Danvers, MA), as well as 60W frosted incandescent bulbs (Loblaws Inc. Calgary, AB). To improve germination and survival, seedlings were

kept under plastic at 100% relative humidity, and at 7DAG plastic was removed and plants were grown at 60% relative humidity.

2.2.2 Identification of Insertion Mutants

DNA was isolated from leaf tissue of each 2-3 week old plant using the CTab protocol. A few young leaves were ground in liquid nitrogen, 300 µL DNA total extraction buffer (Appendix) was added and preps were incubated for 1 hour at 65^{o}C before a chloroform extraction was performed. Supernatant was added to fresh tubes and 2/3 volume of isopropanol was added. DNA was allowed to precipitate for at least two hours at 4^{o}C before preps were washed 2x with ethanol, air dried, and suspended in water.

Primers were designed to flank T-DNA insertion sites (obtained from TAIR, www.arabidopsis.org) using Primer3Plus software (www.bioinformatics.nl/cgi-bin/primer3plus/prime r3plus.cgi). PCR reactions using designed primers and Lbc1 and forward or reverse primer combinations outlined in Table 3 were used to identify plants homozygous for insertions in the genes of interest and self-seed was saved for phenotypic analysis of progeny.

2.2.3 Phenotypic Analysis of Insertion Mutants

SALK_110728 (*arfa1e-2*), SALK 130670 (*arfa1e-1*), SALK_107687 (*arfa1a*), SALK_027659 (*arfa1b*), and SALK_039612 (*arfa1d*), were planted 15 to a pot, cotyledons and first leaves were collected and placed in ethanol for a few hours, then cleared in chloral hydrate (8 chloral hydrate: 2 glycerol: 1 water) for 1 week, before being mounted on a slide in 67% glycerol.

Phenotypic analysis of cotyledons was performed using dark field microscopy and dissecting scope. Cotyledons were classified into 8 different categories annotated X+Y, where X= the number of closed loops, and Y= the number of open loops (Figure 6A). The number of veins, closed loops, distal and proximal non-meeting and gaps (Figure 6B) in wild type and mutant cotyledons were recorded and compared via Student's t-tests where a value of $p<0.05$ represents a significant difference between phenotypes.

2.2.4. Generation of double and triple mutants

Plants homozygous for insertions in ARFA1 family genes were intercrossed and the F2 population of SALK_110728 (*arfA1e-2*) x SALK_107687 (*arfa1a*), as well as SALK_110728 (*arfA1e-2*) x SALK_027659 (*arfa1b*) were screened for double mutants using PCR and primer sets specific to each SALK line (Table 3). Due to time constraints, the first homozygous insertion lines to be identified were the first to be crossed to produce double mutants. Double mutants identified were crossed, producing an F1 that was homozygous for *arfa1e* and heterozygous for *arfa1a* and *arfa1b*. PCR was used to identify triple mutants in the F2 generation.

3. Results

3.1 cDNA library screen

A yeast two-hybrid screen was initiated in order to identify proteins interacting with FKD1 and better define the role of FKD1 in PIN1 localization during vein patterning. The central principle of the yeast two-hybrid is to detect protein interactions between the 'bait' (fusions to GAL4 DB) and 'prey' (fusions to GAL4 TA) proteins, leading to the transcription of reporter genes (Figure 4). This limits the yeast two-hybrid to detecting interactions between proteins that are capable of passing through the nuclear membrane. The putative protein structure of FKD1 (Predict Protein, www.predictprotein.org/) includes a hydrophobic region (amino acids 219-246, Figure 3), which could prevent FKD1 from entering the nucleus by embedding in a membrane. As a result three 'bait' fusions were constructed, one with the full FKD1, and two of which excluded the hydrophobic region; 1) the N-terminal construct, that encompassed the N-terminal region of the DUF828 (amino acids 1-221), and 2) the C-terminal construct, that included the C-terminal of the DUF 828 and the full PH domain (amino acids 246-498)(Figure 3).

Before conducting the cDNA library screens, full FKD1, N-terminal, and C-terminal 'bait' fusions were tested for their ability to activate transcription of *HIS3* and *lacZ* reporter genes in the absence of interaction. None of the FKD1 'bait' fusions activated the *lacZ* reporter gene in yeast, but yeast containing full length FKD weakly grew on –leu-his + 10mM 3AT plates. The small amount of self-activation exhibited by full FKD1 was eliminated when the stringency of the *HIS3* assay was enhanced through raising the 3AT concentration to 15mM (Figure 7B). As a result

15mM 3AT was used in all subsequent *HIS3* assays for all three constructs. 'Bait' fusion proteins also failed to activate reporter genes in negative controls featuring the empty 'prey' vector, and in tests with the 'prey' as cruciferin (Figure 7B), which is a seed storage protein that does not interact with any known proteins (Kohalmi et al., 1998).

FKD1 'bait' fusion proteins (full FKD1, N-terminal, and C-terminal) were used to screen a library of 'prey' fusions for interactions. Interactions between FKD1 and unidentified proteins reconstituted the GAL4 DB and TA to enable transcription of *HIS3* and *lacZ* reporter genes, inducing histidine prototrophy and production of β-galactosidase (detected via X-gal assay) respectively. Initial screens identified 332 histidine prototrophs, 89 from the full length FKD1 screen, 159 from the N-terminal screen, and 84 from the C-terminal screen. When prototrophs were re-screened 20/332 colonies were positive in both HIS3 and X-gal assays, 16 from the full FKD1 screen and 4 from the N-terminal, and these were considered putative FKD1 interacters (Figure 8B). I successfully isolated DNA from 15/20 of the positive yeast, 14 from the full FKD1 screen, and 1 from the N-terminal screen. Following transformation of DNA into *E. coli* and then DNA extraction, DNA preparations with a *SalI*/*NotI* restriction digest pattern different than the 'bait' control were sent for sequencing. Sequences were used as queries against *Arabidopsis* sequence via TAIR BLAST 2.2.8 (Table 4). Several interacters identified in the full FKD1 cDNA library screen are components of stress response systems, such as OXYGEN EVOLVING COMPLEX SUBUNIT 23 (bacterial defense), SENESCENCE 1 (phosphate starvation), EARLY RESPONSIVE TO DEHYDRATION 15 (drought response), ARABIDOPSIS

CYTOCHROME REDUCTASE1 (oxidative stress), and GLYCINE RICH PROTEIN2 (cold response) (TAIR, www.arabidopsis.org). A lipid transfer protein (LTP) was also identified, and such proteins may be secreted during stress response, but also have roles in cutin formation, embryogenesis, and symbiotic interactions (Kader, 1996). At the molecular level LTPs have been implicated in the transfer of phospholipids between membranes (Kader, 1996). This interaction was noteworthy because FKD1 localization is hypothesized to rely on binding of phospholipid signals in TGN membranes (Naramoto et al., 2010). Interaction of the full length FKD1 with ARFA1e, part of a family of proteins involved in coating and uncoating of transport vesicles (Gebbie et al., 2005), was also extremely interesting due to the hypothesized role of FKD1 in vesicle cycling. There were also a couple of proteins identified with general cellular functions such as an Acyl-transferase family protein and an ATPase.

A subset of the interacters identified in the screens using full length FKD1 'bait' are commonly isolated in cDNA library screens (Kohalmi, personal communication), and likely represent false positives, such as UBIQUITIN-CONJUGATING ENZYME 28 (FL116 and FL27), CRUCIFERIN C (FL2), and ribosomal protein of the LTP 41 group (FL38).

3.1.2 Replicating the original library screen

Following sequencing, the 15 'prey' cDNAs isolated from *E. coli* were transformed back into 'bait' containing yeast cells used in initial library screens, in an attempt to replicate the results. Attempts to replicate interactions between full FKD1 and the 14 'preys' listed in Table 4 were unsuccessful (data not shown). To

ensure this was not due to mislabeling of cells prior to shipping from University of Western Ontario to Lethbridge, or a change in the full FKD1 'bait', such as a mutation, binary assays were also performed by simultaneously transforming empty cells with the FKD1 'bait' constructs and cDNA 'preys', and again no interactions were observed (Figure 9). In contrast, re-transformation of X102 (FKD1 fragment) into cells containing N-terminal and Full FKD1 'bait' were positive in both *HIS3* and X-gal assays (Figure 9B). X102 'prey' showed slight activation of *HIS3* in the absence of any 'bait' and no activation of the *lacZ* reporter gene, indicating that results obtained are not likely due to self-activation (Figure 10B).

3.1.3 Testing selected interactions with full-length preys

The cDNAs identified as interacters in the original screen featured partial cDNAs as a product of the oligo-dT primer method described in 2.1.5. Two interacters were selected for testing using full-length cDNAs, ARFA1e (FL13), and FKD1 (X102). I began making 'prey' fusion constructs featuring these cDNAs for testing in binary assays with FKD1 prior to the replication of the original library screens to allow the completion of the project. To compare the ability of different FKD1 protein domains to form homodimers, the FKD1 N-terminal and C-terminal coding regions were also ligated into 'prey' constructs. Prior to testing the FKD1-FKD1 and FKD1-ARFA1e interactions, all new constructs were tested for the ability to activate reporter genes alone or with an empty 'bait' vector, and all tested negative (Figure 10B). Yeast two-hybrid assays featuring full FKD1 and N-terminal 'bait' constructs in combination with newly generated 'preys' all tested negative for interaction.

Partial and full length ARFA1e 'preys' failed to interact in yeast two-hybrid binary assays with either full FKD1 or the N-terminal 'bait' fusions (Figure 9 and Figure 11 respectively). This fits with an inability to replicate the original interaction between full FKD1 and FL13.

It was found that X102 (FKD1 amino acids 58-219, Figure 3) interacted with both the full and N-terminal FKD1 'baits', indicating that the N-terminal is sufficient for the FKD1 homodimer formation. Surprisingly, interactions did not occur between any of the full length FKD1 'bait' and full FKD1, N-terminal or C-terminal 'preys' (Figure 11). There was also no interaction observed between N-terminal 'bait' and N-terminal or C-terminal 'preys' (Figure 11). These results indicate that the inclusion of the first 57 amino acids at the N-terminal in these constructs relative to the X102 'prey' is preventing an interaction.

3.2 Phenotypic analysis of insertion mutants

To verify the biological relevance of selected interactions identified in the yeast two-hybrid library screen, one strategy is to screen for abnormal vascular phenotypes in plants mutant for putative FKD1 interacters. A vascular phenotype would indicate: 1) that the gene is expressed in the same tissues as *FKD1*, and 2) that the protein has similar function to FKD1, which could potentially indicate interaction *in planta*. Identification of novel mutant vascular phenotypes also provides an opportunity to contribute more generally to our understanding of the mechanism of vein patterning in plants.

The SALK institute (La Jolla, CA, USA) has created insertion mutants for 21, 700 out of the 29, 454 genes in the *Arabidopsis thaliana* genome by transforming

plants with *Agrobacterium* transferred DNAs (T-DNAs) that will randomly insert into the genome and interrupt sections of the DNA sequence (Alonso et al., 2003). Typically a T-DNA contains a series of genes involved in manipulating host hormones, such as auxin, to produce a tumor, a center for the production of carbon and nitrogen sources consumed by the *Agrobacterium* (Zupan and Zambryski, 1995). The removal of tumor inducing genes allows for insertion of a minimal T-DNA without altering plant cell differentiation (Zambryski et al., 1983). The insertion of a T-DNA into a promoter, an exon, an intron, and the 5' or 3' UTR is likely to 'knock-out' the function of that DNA element. One advantage of insertion lines is that PCR can be used to detect whether plants carry a wild type or 'knocked-out' form of a gene. Insertion lines in putative interacters AT3G62290 (*ARFA1e*), AT1G56045 (ribosomal protein), AT4G13850 (*GLYCINE RICH PROTEIN2*) were chosen for analysis. As well, I found that *ARFA1e* is part of a family of 6 *ARFA1* genes (*ARFA1a-f*) and exhibits 97-99% amino acids identity with these other family members (TAIR, www.arabidopsis.org). I reasoned that some family members might perform a similar function as ARFA1e, so I analyzed insertions mutants in these genes (*ARFA1a*, *ARFA1b*, *ARFA1c* and *ARFA1d*) in order to assess a possible role in vein patterning.

PCR was used to identify plants homozygous for T-DNA insertions. Primers flanking T-DNA insertion sites listed by ABRC (TAIR, www.arabidopsis.org) recognized the presence of a wild-type allele (Figure 12A), while the presence of an insertion prevents amplification (Figure 12B). Similarly, a second PCR reaction that combines either the forward or reverse primer with a T-DNA insertion specific

primer (Lbc1) detects an insertion through the presence of a PCR product (Figure 12C and D), while the absence of the T-DNA prevents amplification. In summary, if a PCR product results only from the forward + reverse primer combination, the plant is homozygous wild-type; if a product results only from PCR with Lbc1 + the forward or reverse, the plant is homozygous for the insertion; and if there is a product resulting from use of both primer sets, the plant is heterozygous for the insertion (Figure 12).

Due to time constraints, I began the identification of homozygous insertion mutants prior to attempting to replicate the yeast two-hybrid. Homozygous plants were identified in all lines except *ARFA1c*, where non-specific primer binding continually prevented identification of insertions. No vein phenotype was obvious for ribosomal protein or *GRP2* insertions lines. However, I observed a subtle cotyledon phenotype in initial screens of ARFA1e alleles *arfa1e-2* (SALK_ 110728) and *arfa1e-1* (SALK_130670). In combination with the previous identification of a cotyledon phenotype in another *arfa1e* insertion mutant SALK_128880 (5' UTR insertion) by Ceserani et al. 2009, this shifted the focus of the mutant analysis towards the *ARFA1* family member lines.

Cotyledons of homozygous insertion lines *arfa1e-1* (SALK_130670), *arfa1e-2* (SALK_ 110728), *arfa1a* (SALK_107687), *arfa1b* (SALK_027687), and *arfa1d* (SALK_039612), were identified via PCR (Figure 13A), collected, and cleared at 14 DAG for comparison to wild type. Cotyledons were classified into the categories 5+1, 4+2, 4+1, 3+2, 2+3, 4, 3+1, 2+2, 3, 2+1, and 2, where the first number indicates the number of closed loops, and the second number indicates the number of loops

failing to meet at one end or containing a gap, as in Ceserani et al. (2009) (Figure 6A and B). Results were recorded as a percent of cotyledons in each category (Figure 6C and D). Wild type cotyledons usually had 4 veins, with the majority falling into the 3+1, 2+2, and 4 categories (Figure 6C). Among the cotyledons with 4 veins, those with four closed loops displayed the most vascular junctions, and thus the size of this category served as an indicator of vascular meeting.

Neither of the *ARFA1e* mutant alleles (*arfa1e-1* and *arfa1e-2*) examined showed a statistically significant difference in the mean number of veins or closed loops (Student's T-test, $p>0.05$,Table 5), or in proximal and distal non-meeting, or number of gaps (data not shown) when compared to wild type I noticed, however, a trend towards increased vein meeting in *arfa1e-1* and *arfa1e-2*, with 40% and 31% of cotyledons, respectively, with 4 veins making 4 closed loops compared to 16% in wild type. In addition to increased vein meeting, the *arfa1e-1* allele showed higher numbers of cotyledons exhibiting 5 or 6 veins (21.7%) compared to wild type (5.4%) (Figure 6C). The increased severity of the *arfa1e-1* phenotype relative to *arfa1e-2* is likely the result of differences in transcription level and stability correlating with differences in insertion position. Insertion in the last intron, as is the case in *arfa1e-1*, may result in truncation and instability of ARFA1E, while insertion in the promoter, as in *arfa1e-2*, will likely reduce transcript levels but still produce some functional protein.

A subtle mutant phenotype in *arfa1e-1* and *arfa1e-2* encouraged the analysis of the other ARFA1 family members for cotyledon vascular phenotypes. Similar to *arfa1e-1* and *arfa1e-2*, single mutants in *arfa1a*, *arfa1b* and *arfa1d* were not

significantly different from wild type (Table 5). *arfa1b* showed the most similarity to the severe *arfa1e-1* allele, with a slight increase in the number of cotyledons exhibiting 5 or 6 veins (7.4%) compared to wild type (5.4%) (Figure 6C). Single mutants in both *arfa1a* and *arfa1b* continued the trend of increased vein meeting observed in *arfa1e* alleles, with an higher number of cotyledons exhibiting 4 meeting veins (25% and 39%, respectively), when compared to wild type (15%). In contrast to *arfa1b*, *arfa1a*, and *arfa1d* had no cotyledons with more than 4 veins, and *arfa1a* was distinct in that it formed cotyledons with as few as 2 veins. *arfa1d* was unique, as it was the only mutant to exhibit a decrease in the number of cotyledons with 4 veins showing 4 closed loops (12%). The subtle defects to cotyledon vein pattern exhibited by ARFA1 family single mutants, accompanied by their high sequence similarity suggest that these genes may act redundantly.

To test the notion that other ARFA1 family members are acting redundantly with ARFA1e, I generated lines doubly mutant for *ARFA1e* and the two mutants with the most distinct phenotypes(PCR results Figure 13): *arfa1b*, which is the most similar to the strong *arfa1e-1* allele, and *arfa1a*, which was distinct from other family members. The *arfa1e-2* mutant allele was chosen for double mutants because it was available sooner. Unlike *arfa1e-1*, the weak *arfa1e-2* allele showed no increase in cotyledons with 5 or 6 veins compared to wild type. The *arfa1b* allele showed a modest increase (7.4% vs. 5.4% in wild type). Double mutants between *arfa1e-2* and *arfa1b* were analyzed and the number of cotyledons with 5 or 6 veins increased to 21.8% (Figure 6D), providing support for the idea of redundancy. Similarly, although there was no increase in cotyledons with 5 or 6 veins in the

arfa1a or *arfa1e-2* single mutants relative to wild type, *arfa1a arfa1e-2* double mutants showed a modest increase (8.3% vs. 5.4% in wild type, Figure 6D). Double mutants also continued the trend of increased vascular meeting shown by *arfa1a* (25%), *arfa1b* (39%), and *arfa1e-2* (31%) single mutants, but with increased severity. 43% of *arfa1a arfa1e-1* and 48% of *arfa1e-2 arfa1b* double mutant cotyledons with 4 veins also had 4 closed loops (Figure 6D). *arfa1a arfa1e-2* showed a lower percentage of cotyledons with 5 or 6 veins, and a smaller number of cotyledons with 4 closed loops relative to *arfa1b arfa1e-2* and these differences are correlated with a decreased severity of the *arfa1a* phenotype relative to *arfa1b* single mutants. Increased phenotypic severity of double mutant phenotypes relative to single mutants suggests that *ARFA1e* acts redundantly with both *ARFA1a* and *ARFA1b*.

4. Discussion

I initiated a yeast two-hybrid screen to identify proteins interacting with FKD1. Of 332 potential interacters initially identified on the basis of histidine prototrophy, only 20 were capable of activating both the *HIS3* and *lacZ* reporter genes demonstrating the importance of the dual reporter system. Of the 20 interactions only one interaction was confirmed, the interaction between FKD1 and itself, indicating that the remainder were false positives. Despite the identification of ARFA1e as a false positive, a vascular cotyledon phenotype was identified in insertion mutants in this gene and 3 closely related genes (*ARFA1a, ARFA1b, ARFA1d*). A more severe phenotype was observed in doubly mutant plants for pairs of the ARFs, indicating that these proteins may have redundant roles in vascular patterning.

4.1 Formation of FKD1 dimers

The potential ability of FKD1 to dimerize is not surprising given that the formation of homodimers is frequent among other proteins involved in vesicle cycling (Roy et al., 2004, Grebe et al., 2000). Both the full length FKD1 and the N-terminal 'baits' interacted with X102 'prey' in binary yeast two-hybrid assays. X102 was identified as a fragment of FKD1 (amino acids 58-219), specifically a region of the DUF828 domain overlapping with the N-terminal construct (amino acids 1-211)(Figure 3). Interaction of the DUF828 with the full length FKD1 and the N-terminal suggests that FKD1 likely forms homo-dimers through the DUF828 domain, and not the PH domain. As expected, a test for interactions between full FKD1 'bait' or the N-terminal 'bait' with the C-terminal 'prey' were negative, but

unexpectedly, tests for interaction between N-terminal 'bait' and 'prey', full FKD1 'bait' and 'prey', and full FKD1 'bait' with N-terminal 'prey', also tested negative. The failure of the FKD1 N-terminal to interact with the N-terminal or full FKD1 contrasts with the ability of X102 to interact with both fusion proteins, and suggests that the 57 additional amino acids at the N-terminal alter protein interaction. A possible explanation is suggested by the finding that smaller cDNAs allow for production of more fusion protein, and a higher ratio of 'prey' to 'bait' actually increases the level of reporter gene activation (Fields and Sternglanz, 1994). A second explanation is that the presence of the 57 N-terminal amino acids physically prevents interaction from occurring between N-terminal fragments and full FKD1 fusion proteins. Protein prediction software was not able to assign the first 34 amino acids of the N-terminal region as a helical structure or a beta-strand structure (Predict Protein, www.predictprotein.org). The lack of predicted structure, in conjunction with the repetitive sequence in this region, suggests that the N-terminal may form an arm-like structure (Steven Mosimann, personal communication). N-terminal arms have been shown to inhibit homodimer formation by limiting proximity of interacting protein domains (Weldon and Schleif, 2006). A scenario such as this may prevent interaction between two FKD1 proteins with intact N-terminal regions, whereas dimer formation is possible if the N-terminal region of one protein (X102) is eliminated.

A splice variant has been identified for FKD1 that lacks the N-terminal region. The full length FKD1 (AT3G63300.1) is 498 amino acids long, while the isoform (AT3G63300.2) is missing the first 116 amino acids from the N-terminus (TAIR,

www.arabidopsis.org, Figure 3). The interactions of X102 with full FKD1 and N-terminal 'bait' fusions could be permitted by its lack of an N-terminal region and since X102 and AT3G63300.2 lack the same 57 N-terminal amino acids, it could be hypothesized that like X102, AT3G63300.2 could interact with AT3G63300.1.

AT3G63300.2 may post-translationally regulate AT3G63300.1 through the formation of dimers. For example, AT3G63300.2 may act by immobilizing AT3G63300.1 through binding or by interfering with its ability to complex with other proteins, such as SFC, thus exerting a dominant negative effect on the 'wild type' protein. While it is easy to imagine a situation where the smaller isoform might positively regulate the full length FKD1, most smaller 'non-functional' proteins negatively regulate larger ones through dimerization (Staudt and Wenkel, 2011; Tian et al., 2006; Vaart and Schaaf, 2009; Zarei et al., 2001). Regulation of splice variant levels has also been hypothesized to act as a fine control on protein abundance (Zarei et al., 2001). Action of AT3G63300.2 as a negative regulator as opposed to a 'functional' protein fits with its inability to rescue the *fkd1* mutant (Hou et al., 2010). To support the idea that the truncated FKD1 isoform negatively regulates the full length FKD1 through the formation of dimers, an additional yeast two-hybrid experiment could be performed using AT3G63300.2 in the hopes of confirming their interaction. A correlation between increases in AT3G63300.2 levels and decreased FKD1 function could be established by over-expressing AT3G63300.2 in wild-type plants and looking for a *fkd1*-like phenotype that would result from AT3G63300.1 repression.

Due to the ability of a fragment of the FKD1 DUF 828 to interact with full FKD1 and N-terminal fusion proteins it is conceivable that other DUF828 domains could interact, either to form homodimers or heterodimers with other DUF828 proteins. In *Arabidopsis* there are 9 genes that code for DUF828 domains paired with PH domains known as the FKD1 gene family (TAIR, www.arabidopsis.org). The DUF 828 domains have no known function and testing interactions between DUF828 domain proteins could provide evidence for a role of this domain in mediating protein interactions. If an interaction is detected, deletion analysis could be used to determine which residues are responsible for interactions. Testing interactions between FKD1 gene family members and X102, as well as AT3G63300.2 may also be worthwhile, especially in a scenario where interaction with truncated FKD1 could negatively regulate the function of these proteins. No other member of the FKD1 gene family produces splice variants without the N-terminal region, suggesting that a FKD1 isoform may be unique in its ability to interact with DUF828.

4.2 The ARFA1 family acts redundantly to control vein pattern in cotyledons

Class I ARFs, such as ARFA1 family members, are thought to be involved in recruiting cargo proteins and vesicle coats at the golgi, the TGN, and endosome (Jackson and Casanova, 2000). There are two important regulators of ARF function in *Arabidopsis* that have vascular phenotypes, the ARF-GEF *GNOM*, and the ARF-GAP *SFC/VAN3* (Figure 2). Both GNOM and SFC/VAN3 are implicated in establishing wild type PIN1 localization, which is essential to flux of auxin and, by extension, vein pattern formation in the leaf. *gnom* is characterized by increased venation in the leaf margin (Koizumi et al., 2000), while *sfc*/*van3* show decreased venation, vascular

non-meeting, and vascular islands (Deyholos et al., 2000; Koizumi et al., 2005), all defects correlated with abnormal PIN1 localization (Steinmann et al., 1999; Scarpella et al., 2006). GNOM is hypothesized to act on class I ARFs (Trang and Bui et al., 2009) and SFC/VAN3 ARF substrates are unknown, making ARFA1e a viable candidate for interaction with either of these proteins. Despite the inability to replicate an interaction between FKD1 and ARFA1e, analysis of ARFA1 insertion mutants revealed a subtle vascular phenotype, suggesting that this ARF family has a role in vein pattern formation. The ARFA1 family of class I ARFs (ARFA1a-ARFa1f) range from 97-100% amino acid identity to ARFA1e, suggesting that these proteins could act redundantly (Gebbie et al., 2005), an idea supported by the subtle nature of the single mutant phenotype.

Insertion mutant lines *arfa1e-1*, *arfa1e-2*, *arfa1a*, and *arfa1b* showed a trend towards increased vein meeting when compared to wild type. In addition, two of these lines, *arfa1e-1* and *arfa1b*, showed an increased number of cotyledons with 5 or 6 veins compared to wild type (Figure 6C). This is reminiscent of weak *gnom* alleles, *pin1* mutants and leaves treated with low levels of auxin efflux inhibitors (Koizumi et al., 2000; Mattsson et al., 1999; Geldner et al., 2003). The similarity in phenotypes is consistent with the hypothesis that ARFA1 family proteins may have a role in regulating distribution or abundance of auxin transporters, such as PIN1, during vein formation.

Increased severity of vascular phenotype in *arfa1e-1* relative to *arfa1e-2* are not explained by differences in expression pattern, function, or ability of the other ARFs to compensate, as they are alleles of the same gene. Variations in the allele

phenotypes can often be attributed to different levels of transcript production following interruption of the gene in different positions. In this case the stronger *arfa1e-1* phenotype could be attributed to ARFA1e truncation following insertion of T-DNA into an intron, while the *arfa1e-1* weak phenotype could be the result of down-regulation, but not complete absence of ARFA1e transcription. A correlation between phenotypic strength and relative transcript levels could be assessed using RT-PCR.

Increased severity of *arfa1e-1* and *arfa1b* phenotypes relative to *arfa1a*, *arfa1e-2* and *arfa1d* may be occurring for two reasons: 1) Like differences between *arfa1e-1* and *arfa1e-2* alleles, differences in phenotypic variability among single mutants could differ solely base on the amount of functional transcript following insertion (*arfa1* insertion positions outlined in Table 3). 2) *arfa1e* and *arfa1b* may have a more significant role in cotyledon vein pattern formation than *arfa1a* and *arfa1d*. It is possible that these proteins may, despite their high sequence similarity, have very distinct functions and expression patterns, but are capable of acting redundantly when one family member is eliminated, leading to partial 'rescuing' of single mutants and minor vascular defects. Ectopic expression of functionally distinct PIN family proteins has been hypothesized to compensate for the loss of one family member in this way (Vieten et al., 2005).

Subtle single mutant vascular phenotypes and high sequence similarity suggested redundancy among ARFA1 family members. To test this idea, I generated and analyzed double mutants expecting to observe an increase in phenotypic severity relative to single mutants. Double mutants *arfa1e-2 arfa1a* and *arfa1e-2*

arfa1b showed an increase in the percentage of cotyledons with four meeting veins, and in the number of veins compared to wild type and to single mutants, providing evidence for redundancy amongst these genes.

The increased strength of double mutant vascular phenotypes in comparison to single mutants provides some support for the notion that *ARFA1* family genes act redundantly. To further explore this idea, I have crossed double mutants to produce an *arfa1e-2 arfa1a arfa1b* triple mutant, which will be identified by PCR and the phenotypic analysis of progeny will determine whether there is a further increase in veins and vein meeting than that exhibited by single and double mutants. The triple mutant will then be crossed to generate quadruple mutants, which I hypothesize will show a further increase in vein density and meeting. Redundancy can also be tested indirectly through *ARFA1:GUS* constructs which would allow for the observation of temporal and spatial expression patterns of *ARFA1* family members. This would determine whether expression of the genes overlaps during cotyledon vein pattern development in wild type. Examining the expression of constructs in mutants would also allow us to observe any ectopic expression of functional ARFs following a mutation in one or more family members.

4.3 Yeast two-hybrid false positives

The 15 protein interactions identified in the yeast two-hybrid grouped into four main categories, those expressed during stress response (OXYGEN EVOLVING COMPLEX SUBUNIT 23, SENESCENCE 1, EARLY RESPONSIVE TO DEHYDRATION 15, ARABIDOPSIS CYTOCHROME REDUCTASE1, GLYCINE RICH PROTEIN2, and possibly the lipid transfer protein), those involved in membrane dynamics (lipid transfer

protein, FKD1, and ARFA1e), those with broad cellular functions (Acyl-transferase family protein and ATPase), and highly expressed proteins (UBIQUITIN-CONJUGATING ENZYME 28, CRUCIFERIN C, and the ribosomal protein). None of the full FKD1 interactions were confirmed in binary screens. Identification of cruciferin as an interacter was particularly alarming, as cruciferin was used in initial screens as a negative control, and showed no signs of interacting with any of the FKD1 'baits' (Figure 7). This served as an indicator that the full FKD1 screen was likely faulty.

The screen for histidine prototrophs is subjective, selecting for colonies that grow more quickly than their neighbors and, in the absence of true positives, false positives may have been selected. The yeast two-hybrid screen is also very sensitive, and is capable of detecting weak, brief, and sometimes non-specific interactions between proteins. This results in a trade-off between increased sensitivity and an increase in the number of false positives (Criekinge and Beyaert, 1999). The tendency of the yeast two-hybrid to identify false interactions accompanied by a failure to detect some relevant interactions may explain the high incidence of false positives obtained using the full length FKD1 as 'bait'. The ability to confirm interactions between the N-terminal 'bait' as well as the full FKD1 'bait' with X102 (FKD1 fragment) suggests that the problem is not specific to the full FKD1-DB fusion or with the protocol.

Fusions to GAL4 TA and DB may limit accessibility to larger protein interacters contributing to the inability to detect interactions (Fields and Sternglanz, 1994). All the fusions used in this thesis were C-terminal relative to the GAL4 DB or TA, potentially limiting the ability of the N-terminal portion of the fusion proteins to

interact. The N-terminal region of all three FKD1-GAL4 DB fusion proteins encompassed portions of the DUF 828. A region of the DUF 828 (X102) was able to form complexes with other DUF828 containing constructs (N-terminal and full FKD1) indicating the potential importance of the DUF to protein interaction. Limited accessibility to the DUF828 in a C-terminal fusion could lead to false negatives in the original yeast two-hybrid, and an N-terminal fusion to the GAL4 DB may reveal additional interactions.

5. Conclusion

This thesis utilized a yeast two-hybrid system to indentify proteins interacting with FKD1 towards two possible outcomes; 1) identifying previously characterized proteins that complex with FKD1 to provide information about its molecular mechanism, and 2) identifying novel proteins involved in vesicle cycling or vein patterning in general.

Evidence from the yeast two-hybrid suggests that FKD1 proteins may form homodimers, but the interaction between FKD1 proteins is contingent on the absence of a possible N-terminal arm-like structure formed by the first 57 amino acids. FKD1-FKD1 interactions occur between FKD1 'bait' and 'prey' constructs containing the DUF828 domain, supporting our original prediction that the DUF828 is involved in protein-protein interaction. Other than the interaction with itself, no other protein interactions were confirmed, either due to the limitations of the yeast two-hybrid system, or because FKD1 forms very few complexes.

ARFA1e was a false positive identified in the yeast two-hybrid screen. Despite the apparent lack of an interaction with FKD1, a subtle vascular cotyledon phenotype characterized by increased vein number and increased vein meeting was identified in the insertion allele *arfa1e-1*. The *arfa1e-2* allele and mutants in closely related genes (*arfa1a* and *arfa1b*) displayed similar deviations from wild type vein pattern, indicating that these proteins may have a role in vascular patterning. Double mutants showed an increase in phenotypic severity supporting the notion that these proteins are acting redundantly during establishment of cotyledon vein pattern.

References

Abel, S., Theologis, A. (2010). Odyssey of Auxin. Cold Spring Harbor Perspectives in Biology 2 (10): 1-13.

Alonso, J., Stepanova, A., Leisse, T., Kim, C., Chen, H., Shinn, P., Stevenson, D., Zimmerman, J., Brajas, P., Cheuk, R., Gadrinab, C., Heller, C., Jeske, A., Koesema, E., Meyers, C., Parker, H., Prednis, L., Ansari, Y., Choy, N., Deen, H., Geralt, M., Hazari, N., Hom, E., Karnes, M., Mulhollan, C., Ndubaku, R., Schmidt, I., Guzman, P., Aguilar-Henonin, L., Schmid, M., Weigel, D., Carter, E., Marchand, T., Resseeuw, E., Brogden, D., Zeko, A., Crosby, W., Berry, C., Ecker, J. (2003). Genome-wide insertional mutagenesis of Arabidopsis thaliana. Science 301 (5633): 653-657.

Bainbridge, K., Guyomarc'h, S., Bayer, E., Swarup, R., Bennett, M., Mandel, R., Kuhlemeier, C. (2008). Auxin influx carriers stabilize phyllotactic patterning. Genes and Development 22 (6): 810-823.

Bayer, E., Smith, R., Mandel, R., Nakayama, N., Sauer, M., Prusinkiewicz, P., Kuhlemeier, C. (2009). Integration of transport-based models for phyllotaxis and midvein formation. Genes and Development 23 (3); 373-384.

Bennett, M., Marchant, A., Green, H., May, S., Ward, S., Millner, P., Walker, A., Schulz, B., Feldmann, K. (1996). *Arabidopsis AUX1* gene: permease-like regulator of root gravitropism. Science 273 (5277): 948-950.

Berdy, S., Kudla, J., Gruissem, W., Gillaspy, G. (2001). Molecular characterization of At5PTase1, an inositol phosphatase capable of terminating inositol trisphosphate signaling. Plant Physiology 126 (2): 801-810.

Bonifacino, J., Jackson, C. (2003). Endosome-specific localization and function of the ARF activator GNOM. Cell 112 (2): 141-142.

Carland, F., Nelson, T. (2009). CVP2-and CVL1-mediated phophoinositide signaling as a regulator of the ARF GAP SCF/VAN3 in establishment of foliar vein patterns. The Plant Journal 59 (6): 895-907.

Ceserani, T., Trofka, A., Gandotra, N., Nelson, T. (2009). VH1/BRL2 receptor-like kinase ineractions with vascular-specific adaptor proteins VIT and VIK to influence leaf venation. The Plant Journal 57 (6): 1000-1014.

Criekinge, W., Beyaert, R. (1999). Yeast Two-Hybrid: State of the Art. Biological Procedures Online 2 (1): 1-38.

Deyholos, M., Cordner, G., Beebe, D., Sieburth, L. (2000). The *SCARFACE* gene is required for cotyledon and leaf vein patterning. Development 127 (15): 3205-3213.

Dhonukshe, P., Aniento, F., Hwang, I., Robinson, D., Mravec, J., Stierhon, Y-D., Friml, J. (2007). Clathrin-mediated constitutive endocytosis of PIN auxin efflux carriers in *Arabidopsis*. Current Biology 17 (6): 520-527.

Fields, S., Song, O. (1989). A novel genetic system to detect protein-protein interactions. Nature 340 (6230): 245-246.

Fields, S., Sternglanz, R. (1994). The two-hybrid system: an assay for protein-protein interactions. Trends in Genetics 10 (8): 286-292.

Friml, J., Benkova, E., Blilou, I., Wisniewska, J., Hamann, T., Ljung, K., Woody, S., Sandberg, G., Scheres, B., Jurgens, G., Palme, K. (2002a). AtPIN4 mediates sink-

driven auxin gradients and root patterning in *Arabidopsis*. Cell 108 (5): 661-673.

Friml, J., Wisniewska, J., Benkova, E., Mendgen, K., Palme, K. (2002b). Lateral relocation of auxin efflux regulator PIN3 mediates tropism in *Arabidopsis*. Nature 415 (6873): 806-809.

Friml, J., Vieten, A., Sauer, M., Weijers, D., Schwarz, H., Hamann, T., Offringa, R., Jurgens, G. (2003). Efflux-dependant auxin gradients establish the apical-basal axis of *Arabidopsis*. Nature 426 (6963): 147-153.

Gebbie, L., Burn, J., Hocart, C., Willianson, R. (2005). Genes encoding ADP-ribosylation factors in *Arabidopsis thaliana* L. Heyn.; genome analysis and antisense suppression. Journal of Experimental Botany 56 (414): 1079-1091.

Geldner, N., Friml, J., Stierhof, Y-D., Jurgens, G., Palme, K. (2001). Auxin transport inhibitors block PIN1 cycling and vesicle trafficking. Nature 413 (6854): 425-428.

Geldner, N., Anders, N., Wolters, H., Keicher, J., Kornberger, W., Muller, P., Delbarre, A., Ueda, T., Nakano, A., Jurgens, G. (2003). The *Arabidopsis* GNOM ARF-GEF mediates endosomal recycling, auxin transport, and auxin-dependant plant growth. Cell 112 (2):219-230.

Goldberg, J. (1999). Structural and functional analysis of the ARF1-ARFGAP complex reveals a role for coatomer in GTP hydrolysis. Cell 96 (6): 893-902.

Grebe, M., Gadea, J., Steinmann, T., Kientz, M., Rahfeld, J-U., Salchert, K., Koncz, C., Jurgens, G. (2000). A conserved domain of Arabidopsis GNOM protein

mediates subunit interaction and Cyclophilin 5 binding. The Plant Cell 12 (3): 343-356.

Gu, F., Crump, C., Thomas, G. (2001). Trans-golgi network sorting. Cellular and Molecular Life Sciences 58 (8): 1067-1084.

Hou, H., Erickson, J., Meservy, J., Schultz, E. (2010). *FORKED1* encodes a PH domain protein that is required for PIN1 localization in developing leaf veins. The Plant Journal 63 (6): 960-973.

Jackson, T., Brown, F., Nie, Z., Miura, K., Foroni, L., Sun, J., Hsu, V., Donaldson, J., Randazzo, P. (2000). ACAPs are Arf6 GRPase-activating proteins that function in cell periphery. The Journal of Cell Biology 151 (3): 627-638.

Jackson, C., Casanova, J. (2000). Turning on ARF: the Sec7 family of guanine-nucleotide-exchange factors. Trends in Cell Biology 10 (2): 60-67.

Kader, J-C. (1996). Lipid-transfer proteins in plants. Annual Review of Plant Physiology and Plant Molecular Biology 47 (1): 627-654.

Keegan, L., Gill, G., Ptashne, M. (1986). Separation of DNA binding from the transcription-activation function of a eukaryotic regulatory protein. Science 231 (4739): 699-704.

Kitakura, S., Vanneste, S., Robert, S., Lofke, C., Teichmann, T., Tanka, H., Friml, J. (2011). Clathrin mediates endocytosis and polar distribution of PIN auxin transporters in *Arabidopsis*. The Plant Cell 23 (5): 1920-1931.

Kleine-Vehn, J., Dhonukshe, P., Sauer, M., Brewer, P., Wisniewska, J., Paciorek, T., Benkova, E., Friml, J. (2008). ARF GEF-dependant transcytosis and polar delivery of PIN auxin carriers in *Arabidopsis*. Current Biology 18 (7): 526-531.

Kohalmi, S., Nowak, J., Crosby, W. (1997). A practical guide to using the yeast 2-hybrid system. Chapter 4. In: Differentially expressed genes in plants – A bench manual (eds. Harper G, Hansen E), Taylor & Francis, London and Washington: 63-82.

Kohalmi, S., Reader, L., Samack, A., Nowak, J., Haughn, G., Crosby, W. (1998). Identification and characterization of protein interactions using the yeast 2-hybrid system. In: Plant Molecular Biology Manual M1 (eds. Gelvin S, Schiperoort R), Kluwer Academic Publishers, Netherlands : 1-30.

Koizumi, K., Naramoto, S., Sawa, S., Yhara, N., Ueda, T., Nakano, A., Sugiyama, M., Fukuda, H. (2005). VAN3 ARF-GAP-mediated vesicle transport is involved in leaf vascular network formation. Development 132 (7): 1699-1711.

Koizumi, K., Sugiyama, M., Fukuda, H. (2000). A series of novel mutants of *Arabidopsis thaliana* that are defective in the formation of continuous vascular network: calling the auxin signal flow canalization hypothesis into question. Development 127 (15): 3197-3204.

Kramer, E., Bennett, M. (2006). Auxin transport: a field in flux. Trends in Plant Science 11 (8): 382-386.

Lohr, D., Venkov, P., Zlatanova, J. (1995). Transcription regulation in the yeast GAL gene family: a complex genetic network. The Journal of the Federation of American Societies for Experimental Biology 9 (9): 777-787.

Mattsson, J., Sung, Z., Berleth, T. (1999). Responses of plant vascular systems to auxin transport inhibition. Development 126 (13): 2979-2991.

Naramoto, S., Kleine-Vehn, J., Robert, S., Fujimoto, M., Dainobu, T., Paciorek, T., Ueda, T., Nakano, A., Montagu, M., Fukuda, H., Friml, J. (2010). ADP-ribosylation factor machinery mediates endocytosis in plant cells. Proceedings of the National Academy of Sciences 107 (50): 21890-21895.

Naramoto, S., Sawa, S., Koizumi, K., Uemura, T., Ueda, T., Friml, J., Nakano, A., Fukuda, H. (2009). Phosphoinositide-dependant regulation of VAN3 ARF-GAP localization and activity essential for vascular tissue continuity in plants. Development 136 (9): 1529-1538.

Nelson, T., Dengler, N. (1997). Leaf vascular pattern formation. The Plant Cell 9 (7): 1121-1135.

Parry, G., Marchant, A., May, S., Swarup, R., Swarup, K., James, N., Graham, N., Allen, R., Martucci, R., Yemm, A., Napier, R., Manning, K., King, G., Bennett, M. (2001). Quick on the uptake: characterization of a family of plant auxin influx carriers. Journal of Plant Growth Regulation 20 (3): 217-225.

Perez-Gomez, J., Moore, I. (2007). Plant endocytosis: it is clathrin after all. Current Biology 17 (6): R217-R219.

Peter, B., Kent, H., Mills, I., Vallis, Y., Butler, P., Evans, P., McMahon, H. (2004). BAR domains as sensors of membrane curvature: the amphiphysin BAR structure. Science 303 (5657): 495-499.

Reinhart, D., Pesce, E-R., Stieger, P., Mandel, T., Baltensperger, K., Bennett, M., Traas, J., Friml, J., Kuhlemeier, C. (2003). Regulation of phyllotaxis by polar auxin transport. Nature 426 (6964): 255-260.

Richter, S., Geldner, N., Schrader, J., Wolters, H., Stierhof, Y-D., Rios, G., Koncz, C., Robinson, D., Jurgens, G. (2007). Functional diversification of closely related ARF-GEFs in protein secretion and recycling. Nature 488 (7152): 488-493.

Roy, R., Laage, R., Langosch, D. (2004). Synaptobrevin transmembrane domain dimerization-revisited. Biochemistry 43 (17): 4964-4970.

Sachs, T. (1981). The control of patterned differentiation of vascular tissues. Advances in Botanical Research 9: 151-262

Sachs, T. (1989). The development of vascular networks during leaf development. Current Topics in Plant Biochemistry and Physiology 8: 168-183.

Sachs, T. (1991). Cell polarity and tissue patterning in plants. Developmental Supplement 1: 83-93.

Scarpella, E., Marcos, D., Friml, J., Berleth, T. (2006). Control of leaf vascular patterning by polar auxin transport. Genes and Development 20 (8): 1015-1027.

Scheffzek, K., Ahmadian, M., Wittinghofer, A. (1998). GTPase-activating proteins: helping hands to complement an active site. Trends in Biochemical Sciences 23 (7): 257-262.

Schiestl, R., Gietz, R. (1989). High efficiency transformation of intact yeast cells using single stranded nucleic acids as a carrier. Current Genetics 16 (5-6): 339-346.

Schmid, S. (1997). Clathrin-coated vesicle formation and protein sorting: an integrated process. Annual Review of Biochemistry 66 (1): 551-548.

Sieburth, L., Muday, G., King, E., Benton, G., Kim, S., Metcalf, K., Meyers, L., Seamen, E., Norman, J. (2006). *SCARFACE* encodes an ARF-GAP that is required for normal

auxin efflux and vein patterning in *Arabidopsis*. The Plant Cell 18 (6): 1396-1411.

Staudt, A-C., Wenkel, S. (2011). Regulation of protein function by 'microProteins'. European Molecular Biology Organization 12 (12): 35-42.

Steinmann, R., Geldner, N., Grebe, M., Mangold, S., Jackson, C., Paris, S., Galweiler, L., Palme, K., Jurgens, G. (1999). Coordinated polar localization of auxin efflux carrier PIN1 by GNOM ARF-GEF. Science 286 (5438): 316-318.

Steynen, Q., Schultz, E. (2003). The FORKED genes are essential for distal vein meeting in *Arabidopsis*. Development 130 (19): 4695-4708.

Suzl, T., Garcia-Mata, R., Brandon, E., Shestopal, S., Alvarez, C., Sztul, E. (2005). Dissection of membrane dynamics of the ARF-guanine nucleotide exchange factor GBF1. Traffic 6 (5): 374-385.

Swarup, R., Kargul, J., Marchant, A., Zadik, D., Rahman, A., Mills, R., Yemm, A., May, S., Williams, L., Millner, P., Tsurumi, S., Moore, I., Napier, R., Kerr, I., Bennett, M. (2004). Structure-function analysis of the presumptive *Arabidopsis* auxin permease AUX1. The Plant Cell 16 (11): 3069-3083.

Szopa, J., Sikorski, F. (1995). ARF-protein antisense potato displays stable ADP-ribosylation of 40 kDa protein. Journal of Plant Physiology 145 (3):383-386.

Tian, W., Fu, Y., Wang, D., Cohen, D. (2006). Regulation of TRPV1 by novel renally expressed rat TRPV1 splice variant. American Journal of Renal Physiology 290 (1): F117-F126.

Trang Bui, Q., Golinelli-Cohen, M-P., Jackson, C. (2009). Large Arf1 guanine nucleotide exchange factors: evolution, domain structure, and roles in

membrane trafficking and human disease. Molecular Genetics and Genomics 282 (4): 329-350.

Vaart, M., Schaaf, J. (2009). Naturally occurring C-terminal splice variants of nuclear receptors. Nuclear Receptor Signalling 7: 1-15.

Vieten, A., Vanneste, S., Wisniewska, J., Benkova, E., Benjamins, R., Beeckman, T., Luschnig, C., Friml, J. (2005). Functional redundancy of PIN proteins is accompanied by auxin-dependant cross-regulation of PIN expression. Development 132 (20): 4521-4531.

Weldon, J., Schleif, R. (2006). Specific interactions by the N-terminal arm inhibit self-association of the AraC dimerization domain. Protein Science 15 (12): 2828-2835.

Wenzel, C., Schuetz, M., Yu, Q., Mattsson, J. (2007). Dynamics of *MONOPTEROS* and PIN-FORMED1 expression during leaf vein pattern formation in *Arabidopsis thaliana*. The Plant Journal 49 (3): 387-398.

Xiao, W., Poirier, M., Bennett, M., Shin, Y-K. (2001). The neuronal t-SNARE complex is a parallel four-helix bundle. Nature Structural Biology 8 (4): 308-311.

Zarei, M., Zhu, N., Alioua, A., Eghbali, M., Stefani, E., Toro, L. (2001). A novel MaxiK splice variant exhibits dominant-negative properties for surface expression. The Journal of Biological Chemistry 276 (19): 16232-16229.

Zambryski, P., Joos, H., Genetello, C., Leemans, J., Van Montagu, M., Schell, J. (1983). Ti plasmid vector for the introduction of DNA into plant cells without alteration of their normal regeneration capacity. European Molecular Biology Organization 2 (12): 2143-2150.

Zazimalova, E., Murphy, A., Yang, H., Hoyerova, K., Hosek, P. (2010). Auxin transporters—why so many? Cold Spring Harbor Perspectives in Biology 2(3): 1-14.

Zupan, J., Zambryski, P. (1995). Transfer of T-DNA from *Agrobacterium* to the plant cell. Plant Physiology 107 (4): 1041-1047.

Table 1. Yeast two-hybrid bait and prey constructs and relevant construction information. Column 1 lists the names of the final fusion constructs, column 2 indicates the vector backbone; PBI-770 (bait vector) or PBI-771 (prey vector), column 3 indicates the cDNA from which the inserts were amplified; U16276 or U12397, column4 indicates the size of the PCR amplified insert, column 5 lists the primer pair names, column 6 lists forward and reverse primer sequences; underlined text represents restriction sites (*SAL1* in forward primer, *NOTI* in reverse primer), stop codons are bolded, and engineered stop codons are bolded and italicized, column 7 lists optimal annealing temperatures for primer sets using Phusion polymerase.

Construct name	**Vector**	**cDNA**	**Size of insert**	**Primer**	**Sequence (5' to 3')***	**Tm**
FKD full length	PBI-770	U16276	1500bp	Y2H_FulllengthFKD_F	GAGAGTCGACGGATGGAGAGAGAACTC	57°C
				PHFulllength_R	AAAGCGGCCGC**TTA**AGGTGCCATCCAT	
FKD N-terminal	PBI-770	U16276	680bp	Y2H_FulllengthFKD_F	GAGAGTCGACGGATGGAGAGAGAACTC	54°C
				NewY2HXdomain_R	AACAGCGGCCGC***CTA***GTGAACCTGTGCATT	
FKD C-terminal	PBI-770	U16276	786bp	Y2H_FKDDUF828/PH_F	GCTTGTCGACCTGGTAAGAACGAGCAG	59°C
				PHFulllength_R	AAAGCGGCCGC**TTA**AGGTGCCATCCAT	
FKD full length	PBI-771	U16276	1500bp	Y2H_FulllengthFKD_F	GAGAGTCGACGGATGGAGAGAGAACTC	57°C
				PHFulllength_R	AAAGCGGCCGC**TTA**AGGTGCCATCCAT	
FKD N-terminal	PBI-771	U16276	680bp	Y2H_FulllengthFKD_F	GAGAGTCGACGGATGGAGAGAGAACTC	54°C
				NewY2HXdomain_R	AACAGCGGCCGC***CTA***GTGAACCTGTGCATT	
FKD C-terminal	PBI-771	U16276	786bp	Y2H_FKDDUF828/PH_F	GCTTGTCGACCTGGTAAGAACGAGCAG	59°C
				PHFulllength_R	AAAGCGGCCGC**TTA**AGGTGCCATCCAT	
ARFA1e	PBI-771	U12397	585bp	AT3G62290fullY2H_F	TCGCCGGGTCGACAAATGGGTCTATC	70°C
				AT3G62290fullY2H_R	AAAAGCGGCCGC**CTA**AGCCTTGTTTG	

Table2. 'Bait' and 'prey' specific primers used to sequence the MCS of PBI-770 and PBI-771 fusion constructs. Forward primers are annotated BC and the reverse primer is the same for both vectors, annotated JN. Melting temperatures were provided by IDT.

Vector	Primer	Sequence (5' to 3')	Tm
PBI-770 'bait'	BC 293	GAATAAGTGCGACATCATC	48.4°C
	JN 069	TTGATTGGAGACTTGACC	49.0°C
PBI-771 'prey'	BC 304	CTATTCGATGATGAAGATACC	47.7°C
	JN 069	TTGATTGGAGACTTGACC	49.0°C

Table 3. Insertion lines (column 1) in genes (column 2) whose products were identified as interacting with FKD1 in the original yeast two-hybrid experiment (AT1G67045, AT4G13850, AT3G62290), as well as ARFA1 family members (AT1G23490, AT5G14670, AT2G47170, AT1G70490). Insertion location (column 3) was obtained from the ABRC website (www.arabidopsis.org), and forward and reverse primers and sequences listed in columns 4 and 5 were constructed with Primer3 Plus to flank T-DNA insertion sites. Primer combinations and optimal annealing temperatures (column 6) used in genotyping (identification of homozygotes indicated by √ in column 7) using Taq Polymerase. Lbc1 sequence noted below.*

Insertion Line	Gene	Insertion Location	Primer	Sequence (5' to 3')	Optimal Tm (°C)	Hom
CS873153	AT1G56045 (ribosomal)	2nd exon	SAIL320WIS278F	TTCATCGATAATACCCATTCATGT	F+R=53 F+Lbc1=53	√
			SAIL320WIS278R	AAAAGGTTTGCTAGAAGAAAGAAAAA		
CS850247	AT1G56045 (ribosomal)	2nd exon	SAIL320WIS278F	TTCATCGATAATACCCATTCATGT	F+R=53 R+Lbc1=53	√
			SAIL320WIS278R	AAAAGGTTTGCTAGAAGAAAGAAAAA		
SALK_ 059714	AT4G13850 (GRP2)	2nd exon	SALK059714F	CAAACTCGGTGGTCTATTGAGA	F+R=53 F+Lbc1=53	√
			SALK059714R	AGCAGGATTCACTCGGATGT		
SALK_135802	AT4G13850 (GRP2)	1st intron	SALK059714F	CAAACTCGGTGGTCTATTGAGA	F+R=53 F+Lbc1=53	√
			SALK059714R	AGCAGGATTCACTCGGATGT		
SALK_130670 (*arfa1e-1*)	AT3G62290 (ARFA1e)	Last intron	SALK130670F	TTGTTTGCTTGCTCATCCAG	F+R=55 F+Lbc1=55	√
			SALK130670R	TTGATGACATATAGGAATCAAAATACG		
SALK_110728 (*arfa1e-2*)	AT3G62290 (ARFA1e)	promoter	SALK128880F2	CGATCGGCCATGTTCTATAAG	F+R=53 Lbc1+R=55	√
			SALK128880R	TTGCAGCATTCATATGGAATAAA		
SALK_107687 (*arfa1a*)	AT1G23490 (ARFA1a)	5' UTR	SALK107687F	TTTGAGAGCAAATGTGTTTTTG	F+R=53 F+Lbc1=58	√
			SALK_107687_R	CAATCCCATCCTGCTTCACT		
SALK_027659 (*arfa1b*)	AT5G14670 (ARFA1b)	5' UTR	SALK_027659_F	CATCGTTTCTCAAAATCTCTGG	F+R=53 F+Lbc1=60	√
			SALK_027659_R	CCACAAGGGACGAATCTGTT		
SALK_135703 (*arfa1c*)	AT2G47170 (ARFA1c)	5' UTR	SALK_135703_F	AACTCGGTTTTGGCTGGTTA	F+R=53 F+Lbc1=53	-
			SALK_135703_R	CAAGACCTTTGTGGACCTACG		
SALK_039612 (*arfa1d*)	AT1G70490 (ARFA1d)	2nd intron	SALK_039612_F	CCATACCTTGTCCTGACCC	F+R=53 F+Lbc1=53	√
			SALK_039612_R	GGGTCAGGACAAGGTATGGA		

*Lbc1 insertion specific primer sequence : 5' CGTCCGCAATGTGTTATTAAG 3'

Table 4. Identities of 15 of 20 putative protein interacters identified in yeast two-hybrid cDNA library screens using either the full length FKD or the FKD1 N-terminal as 'bait'. Column 1 denotes the 'bait' used, column2 is the given prey cDNA name prior to identification, column 3 is the locus of interacters following sequencing and identification via TAIR BLAST 2.2.8, column 4 is a description of known protein function.

'Bait'	Prey cDNA	Locus*	Description**
Full Length	FL1	AT4G24520	ATR1 (ARABIDOPSIS CYTOCHROME REDUCTASE1)
	FL2	AT4G28520	CRC (CRUCIFERIN C), seed storage protein
	FL3	AT5G25460	Unknown protein, member of the DUF642 superfamily
	FL6	AT1G06680	OE23 (OXYGEN EVOLVING COMPLEX SUBUNIT 23), photosystem II
	FL13	AT3G62290	ARFA1e (ADP-RIBOSYLATION FACTOR A1E), GTPase family protein
	FL27	AT1G64230	UBC28 (UBIQUITIN-CONJUGATING ENZYME 28)
	FL34	AT4G00895	ATPase
	FL37	AT2G10940	Uncharacterized lipid transfer protein
	FL38	AT1G56045	Ribosomal protein, L41 family
	FL39	AT2G41430	ERD15 (EARLY RESPONSIVE TO DEHYDRATION15), stress response protein
	FL40	AT4G35770	SEN1 (SENESCENCE 1), senescence-associated, induced by phosphate starvation
	FL41	AT3G48720	Acyl-transferase family protein
	FL44	AT4G13850	GRP2 (GLYCINE RICH PROTEIN2), glycine rich RNA binding protein
	FL116	AT1G64230	UBC28 (UBIQUITIN-CONJUGATING ENZYME 28)
N-terminal	X102	AT3G63300	FKD1 (FORKED1)

*TAIR BLAST 2.2.8 (http://www.arabidopsis.org/Blast/index.jsp)
**description from TAIR (http://www.arabidosis.org)

Table 5. Mean number of veins and closed loops (column 1) in cotyledons for wild type (column2), ARFA1 family single mutants (*arfa1e-1*, *arfa1e-2*, *arfa1a*, *arfa1b*, and *arfa1d*, columns 3-7), and double mutants (*arfa1a arfa1e-2* and *arfa1b arfa1e-2*, columns 8 and 9). Sample size indicated in brackets in row 1. Student's t-tests comparing wild type to each genotype were applied, and no significant differences were found ($p<0.05$).

Character	**Wild Type (n=129)**	***arfa1e-1* (n=23)**	***arfa1e-2* (n=14)**	***arfa1a* (n=35)**	***arfa1b* (n=27)**	***arfa1d* (n=30)**	***arfa1a arfa1e-2* (n=48)**	***arfa1b arfa1e-2* (n=55)**
Number of veins	3.8 ± 0.6	4.1 ± 0.8	3.9 ± 0.3	3.6 ± 0.6	3.8 ± 0.5	3.9 ± 0.3	3.9 ± 0.5	4.3 ± 0.6
Number of closed loops	2.8 ± 0.7	3.0 ± 0.2	3.0 ± 0.8	2.7 ± 0.8	3.0 ± 0.8	2.6 ± 0.7	3.2 ± 0.6	3.4 ± 0.7

Figures

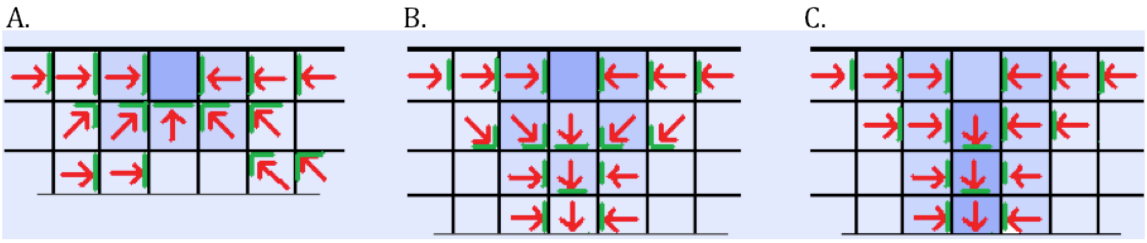

Figure 1. Model for changes in PIN1 membrane localization (green) and hypothesized changes in auxin flux (red arrow) and concentration (blue shading, where dark blue = high auxin and light blue = low auxin) during the development of the midvein presented by Bayer et al. (2009). **A.** Establishment of auxin maxima at the leaf tip (dark blue) is correlated with epidermal localization of PIN1 to membranes facing the leaf tip. **B.** High auxin at the leaf tip is correlated with a shift to lateral, oblique, and basal PIN1 localization away from the auxin maxima, initiating the basal auxin flux that will specify the midvein. **C.** Loss of oblique PIN1 localization and a shift to only lateral and basal localization down the incipient midvein drains auxin from the leaf tip and surrounding tissues, leading to high flux in a narrow field of cells that will form the midvein.

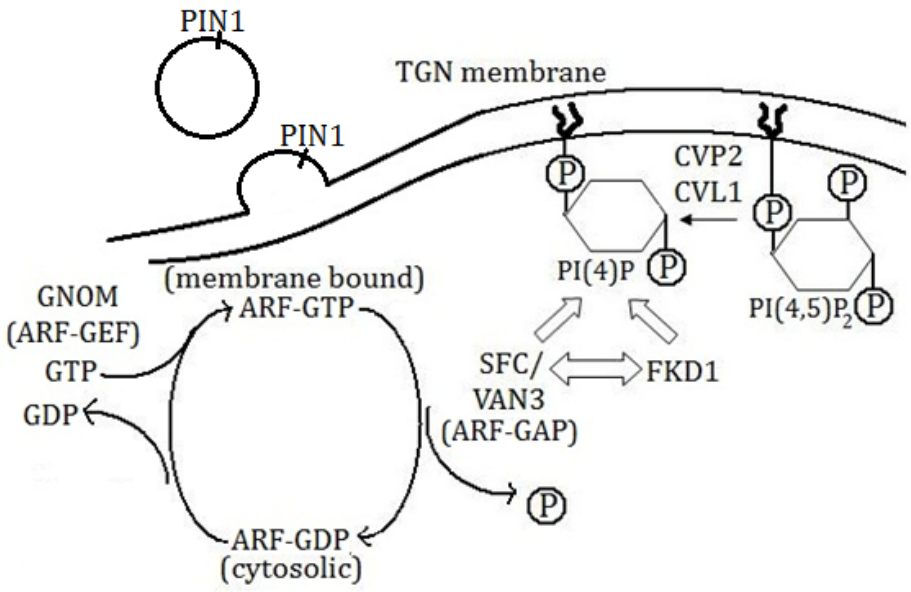

Figure 2. A hypothetical model depicting the mechanism by which PIN1 containing vesicles are formed. A yet unidentified TGN-localized ARF cycles between GTP and GDP bound forms. The model assumes that both the ARF-GEF GNOM, and the ARF-GAP SFC are acting on this ARF. GNOM replaces GDP with GTP, ARF-GTP becomes bound to the donor membrane and recruits vesicle coat proteins, such as clathrin, to a newly forming vesicle containing cargo proteins such as PIN1. Following the budding of the vesicle, fusion with a target cell membrane requires the dissociation of the vesicle coat, triggered by SFC catalyzed hydrolysis of GTP to produce ARF-GDP. Recruitment of SFC/VAN3 and its protein partner FKD1 to the Trans-Golgi Network (TGN) occurs through the recognition of PI(4)P embedded in the compartment membrane. The inositol phosphate 5' – phosphatases CVP2 and CVL1 produce PI(4)P.

A.

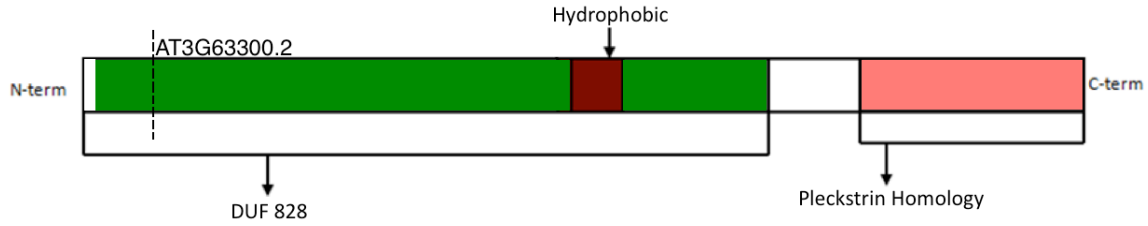

B.

{Met E R E L R R P N P I N S S R R P E I F S S G G S S T Q L P E S P R G P 36
AT3G63300.1
Met E F L S R S W S V S A L E V S R A L H T [A K S A S A T N R P P S S I N T 73

P I P E E T L N P E K E E C P P E N S T S V S S Q F S F A A S A T S Q L V L E 112

R I Met S Q S E V S P L T S G R L S H S S G P L N G G G S F T E T D S P P I 149
Met K AT3G63300.2
S P S D E F D D V I K Y F R T H N T I H P L F S G T G G S R G T T G N G S N 187

T P Met A G T G P K T V G R W L K D R K E K K K E E T R T Q N A Q] V H} A 222

A V S V A A V A S A V A A V A A A T A A S S P <G K N E Q Met A R I D Met A 257

Met A S A A A L V A A Q C V E A A E I Met G A D R D H L T S V V S S A V N V 276

K S H D D I V T L T A A A A T A L R G A A T L K A R A L K E V W N I A A V L P 332

A E K G A S S A L C G Q V D T K H S D S S F S G E L P V A G E D F L G V C 369

N Q E L L A K G T E L L K R T R G G E L H W K I V S V Y I N K A G Q A V L K 407

Met K S K H V G G T F T K K K K H Met V L E V R K D I P A W A G R D L F N G 443

D K H H Y F G L K T E T K R V I E F E C R N Q R E Y E I W T Q G V S R L L A I 482

A A E K K Q K S S Met S K W Met A P Stop> 498

Figure 3. A. Schematic of full length FKD1 (AT3G63300.1) putative protein domains, and **B.** amino acid sequence. **A.** FKD1 is predicted to contain two putative protein domains (Predict Protein, http://www.predictprotein.org/) based on amino acid similarity to characterized protein domains; a Domain of Unknown Function 828 (green) with a hydrophobic domain (maroon), and a Pleckstrin Homology domain (pink). Alternative splicing produces a FKD1 isoform, AT3G63300.2, denoted with a dashed line. **B.** Amino acids (color corresponding to protein structures in **A.**)contained within the putative protein domains: DUF828 (green, amino acids 30-337) and the Pleckstrin Homology domain (pink, amino acids 375-498); the hydrophobic region is indicated in maroon (amino acids 219-245). Portions of protein used in yeast two-hybrid experiments are outlined using brackets: N-terminal domain, amino acids 1-221 by {}, X102, amino acids 58-219 by [], and C-terminal domain, amino acids 246-498 by <>. The first two amino acids of a splice variant (AT3G63300.2) are listed below line 4 and amino acids shared by both protein isoforms begin at the vertical dashed line (amino acid 118). Amino acid number shown along the right side.

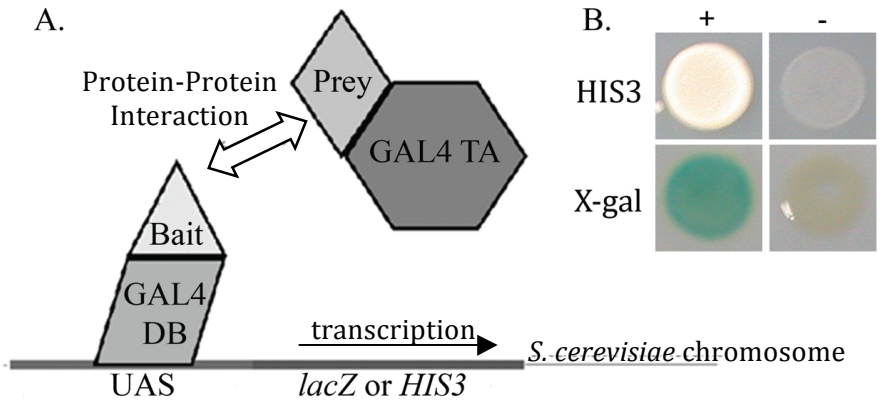

Figure 4. A. Yeast two-hybrid schematic showing the GAL4 DNA binding domain (DB) 'bait' fusion protein interacting with a 'prey' protein fused to the GAL4 activation domain (TA) (Modified from Kohalmi et al., 1997). Interaction between the FKD1 bait and the prey protein activates the transcription of *lacZ* or *HIS3* reporter genes regulated by the GAL4 Upstream Activation Sequence. In the absence of interaction reporter genes are not transcribed. **B.** Left column, a positive control (AGL4-T4) exhibiting activation of *HIS3* (row1) and *lacZ* reporter genes (row2). Right column, negative control (AGL4-T7 + an empty DB) lacking reporter activation.

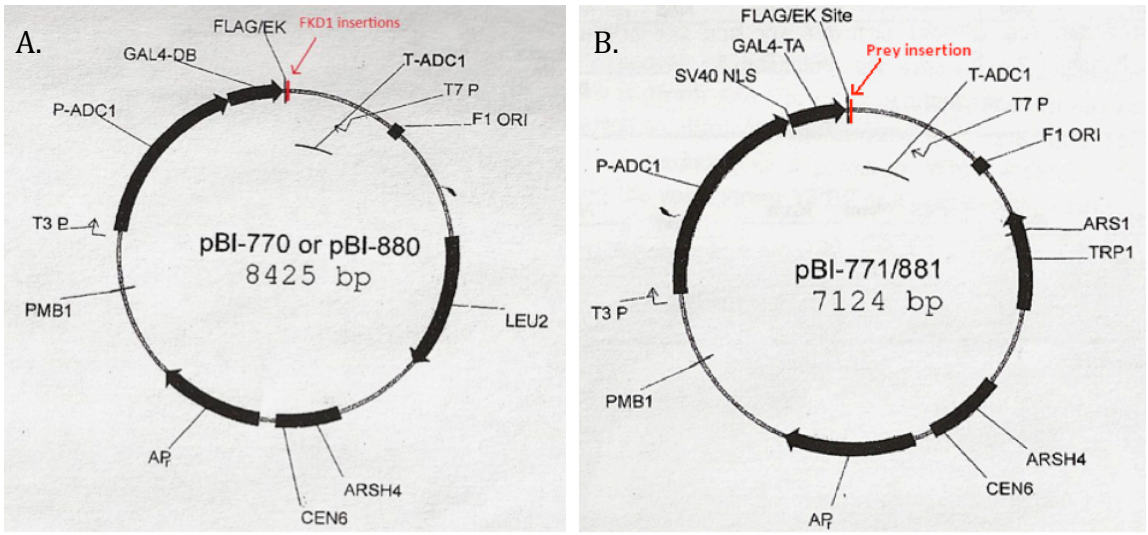

Figure 5. Yeast – *E. coli* shuttle vectors PBI-770 and PBI-771 (modified from Kohalmi et al., 1998. **A.** PBI-770 vector was utilized for expression of the FKD1 cDNA fragments fused to the C-terminal of the yeast GAL4 DNA binding domain (DB) in the yeast two-hybrid system to generate 'bait' fusion proteins. **B.** PBI-771 vector was utilized for expression of the cDNA library and full length 'prey' cDNAs fused to the C-terminal of the yeast GAL4 transcription activation domain (TA) in the yeast two-hybrid system to generate 'prey' fusion proteins. **A., B.** Insertion sites of the FKD1 and preys are denoted by arrows, and follow the FLAG/EK sequence.

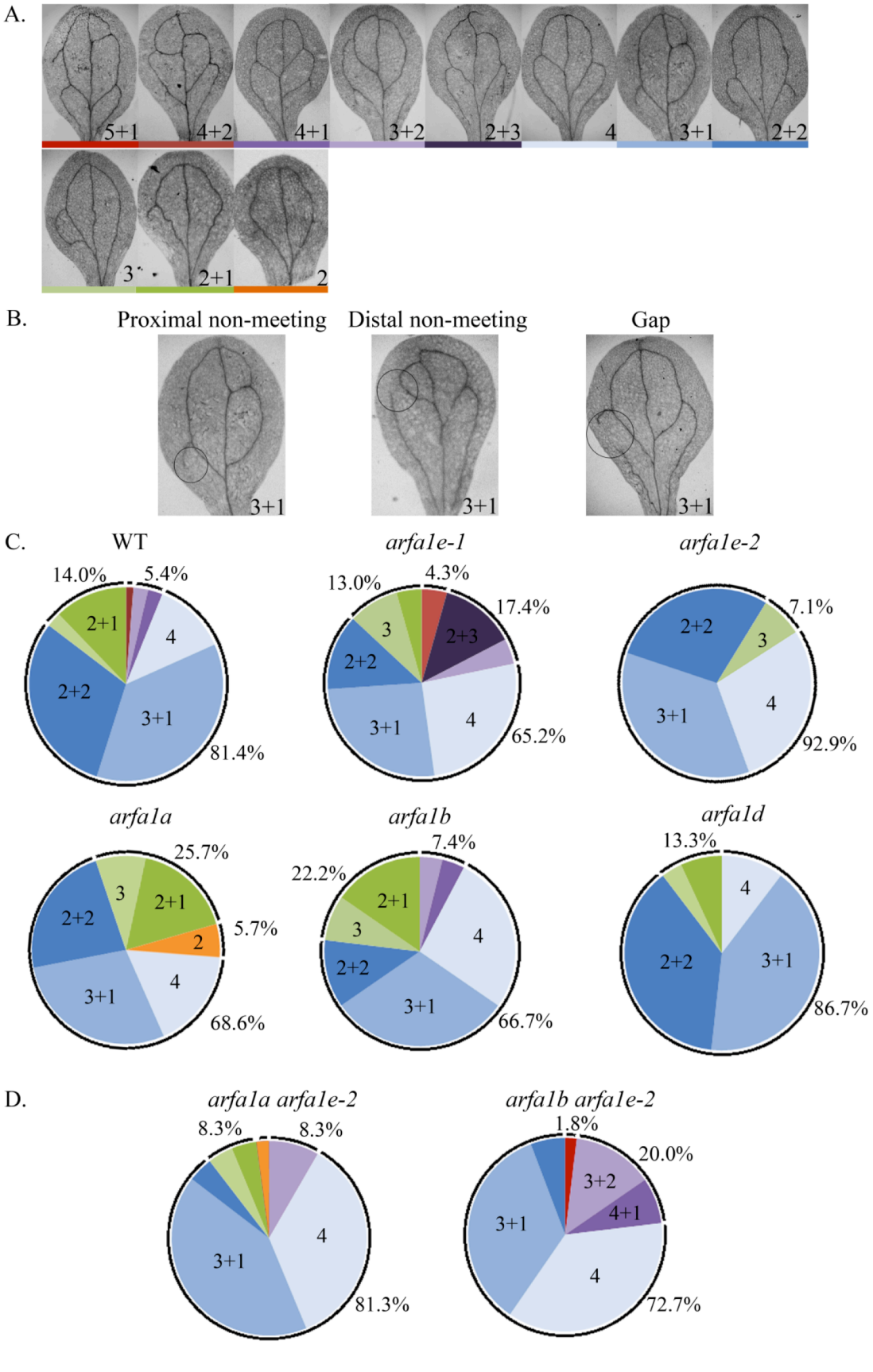
A.
5+1
4+2
4+1
3+2
2+3
4
3+1
2+2
3
2+1
2
B.
Proximal non-meeting
Distal non-meeting
Gap
3+1
3+1
3+1
C.
WT
14.0%
5.4%
2+1
4
2+2
3+1
81.4%
arfa1e-1
13.0%
4.3%
17.4%
3
2+3
2+2
3+1
4
65.2%
arfa1e-2
7.1%
2+2
3
3+1
4
92.9%
arfa1a
25.7%
3
2+1
2+2
5.7%
2
4
3+1
68.6%
arfa1b
7.4%
22.2%
2+1
3
4
2+2
3+1
66.7%
arfa1d
13.3%
4
2+2
3+1
86.7%
D.
arfa1a arfa1e-2
8.3%
8.3%
4
3+1
81.3%
arfa1b arfa1e-2
1.8%
20.0%
3+2
4+1
3+1
4
72.7%

Figure 6. Vascular phenotypes in ADP-RIBOSYLATION FACTOR1 family mutant cotyledons. **A.** Phenotypes of cotyledons classified by the number of closed loops vs. the number of open loops as in Cesarani et al. (2009). Number in the bottom right represents the number of closed loops + open loops, and the color at the base of the image corresponds to colors in graphs in **C.** and **D. B.** Examples of proximal and distal non-meeting and gaps in cotyledons with four veins exhibiting three closed loops and one open (3+1). **C.** Graphs showing percentage of cotyledons in different categories of ARFA1 insertion mutants, *arfa1e-1* (n=23*), arfa1e-2* (n=14), *arfa1a* (n=35), *arfa1b* (n=27) and *arfa1d* (n=30) in comparison to wild type (n=129) cotyledons at 14 DAG. Colors represent cotyledons within each of the phenotypic categories shown in **A.** Phenotypic categories are grouped according to the total number of veins, and percent of cotyledons in each group are outlined in black. **D.** Phenotypic analysis of double insertion mutants *arfa1a*/*arfa1e-2* (n=48), and *arfa1b arfa1e-2* (n=55). Colors represent the proportion of cotyledons fitting into each of the phenotypic categories shown in **A.** black outlines group categories according to the total percentage of cotyledons with the same number of veins.

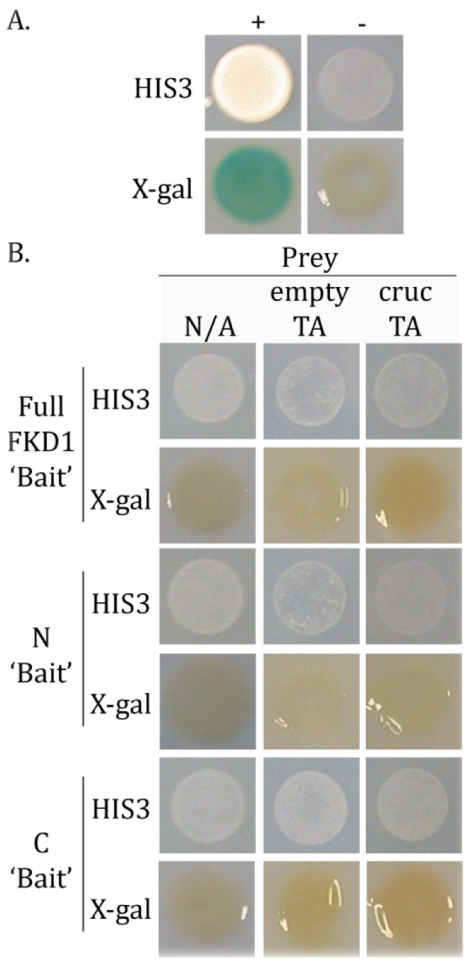

Figure 7. Yeast two-hybrid 'bait' negative controls **A.** Left column, a positive control (AGL4-T4) exhibiting activation of *HIS3* (row1) and *lacZ* reporter genes (row2). Right column, a negative control (AGL4-T7 + an empty DB) lacking *HIS3* and *lacZ* reporter activation. **B.** Column 1, test for self-activation of reporter genes by 'bait' only; full FKD1 (row1 and 2), the N-terminal (rows 3 and 4), and the C-terminal (rows 5 and 6). Column 2, test for activation in the presence of FKD1 'bait' fusions and an empty TA ('prey') vector. Column 3, test for an interaction between FKD1 'bait' fusions with a cruciferin 'prey' fusion. HIS3 assays assessed growth on histidine free media + 15mM 3AT at 28^{o}C after 4 days and X-gal assays incubated for 4hours at 28^{o}C on 2 day old cells grown at 28^{o}C.

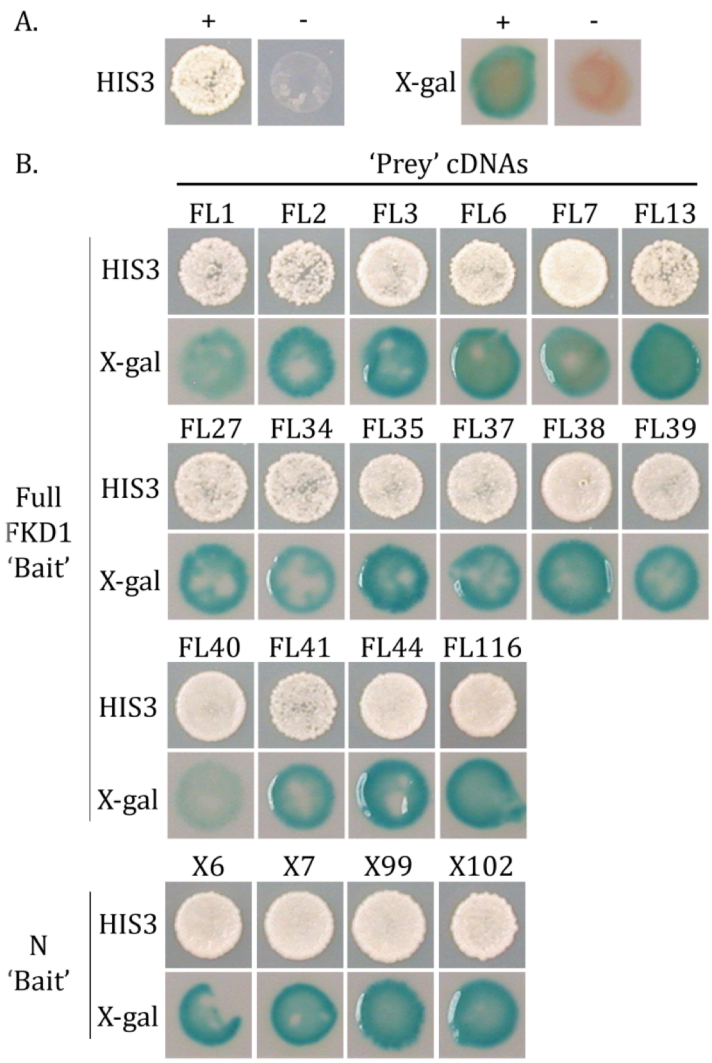

Figure 8. Assays for protein-protein interaction between full FKD1 or the FKD1 N-terminal and putative interacters. **A.** Positive control (AGL4-T4) exhibiting activation of *HIS3* (column1) and *lacZ* reporter genes (column3). Negative control (AGL4-T7 + an empty DB) lacking *HIS3* activation (column2) or *lacZ* activation (column4). **B.** Activation of both *HIS3* (rows 1, 3, 5, 7) and *lacZ* (rows 2, 4, 6, 8) reporter genes in the presence of a full FKD1 or N-terminal 'bait' fusion protein and 20 unidentified 'prey' cDNA fusions. HIS3 assays assessed growth on histidine free media + 15mM 3AT at 28^{o}C after 4 days and X-gal assays incubated for 4hours at 28^{o}C on 2 day old cells grown at 28^{o}C.

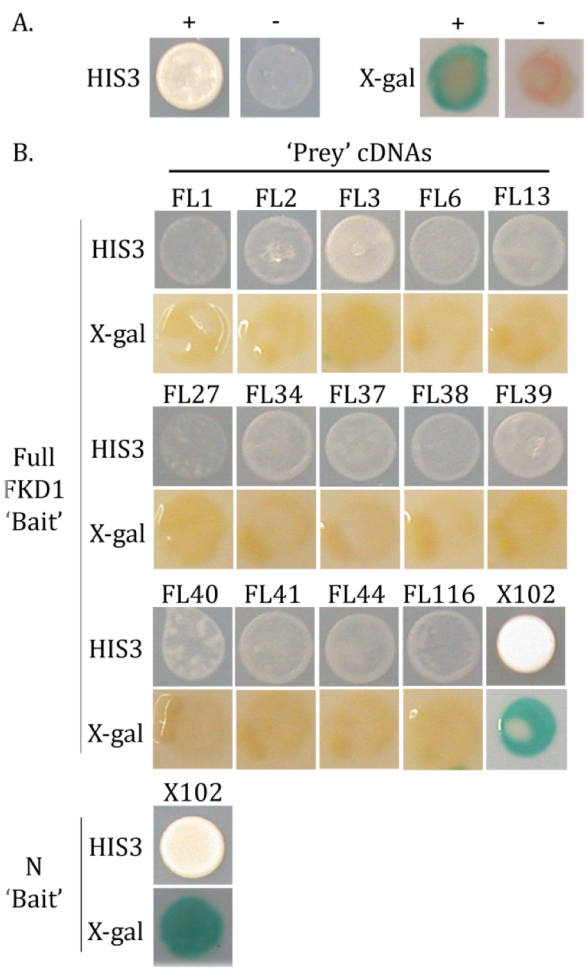

Figure 9. Binary yeast two-hybrid assays for protein-protein interaction following simultaneous transformation of empty yeast with full FKD1 or the FKD1 N-terminal 'bait' and 15/20 'preys' from original screens. **A.** Positive control (AGL4-T4) exhibiting activation of *HIS3*(column1) and *lacZ* reporter genes (column3). Negative control (AGL4-T7 + an empty DB) lacking *HIS3* activation (column2) or *lacZ* activation (column4). **B.** 14/15 binary assays using full length FKD1 as 'bait' were negative for interaction. X102 'prey' showed interaction with both the full length FKD1 (row 5 and 6, column 5) and the N-terminal 'baits' (rows 7 and 8, column1). HIS3 assays shown in rows 1, 3, 5, 7, X-gal assays in rows 2, 4, 6, 8. HIS3 assays assessed growth on histidine free media + 15mM 3AT at 28^{o}C after 4 days and X-gal assays incubated for 4 hours at 28^{o}C on 2 day old cells grown at 28^{o}C.

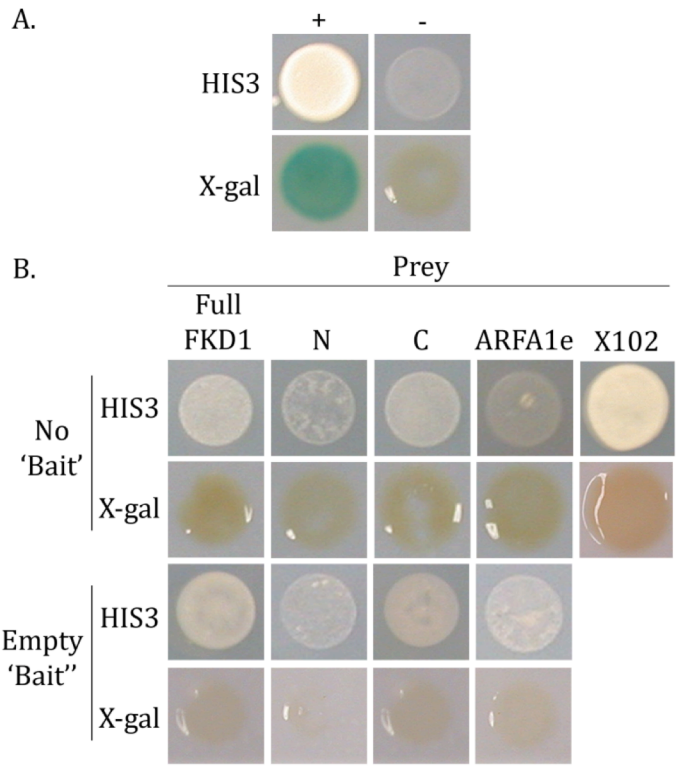

Figure 10. Yeast two-hybrid 'prey' negative controls **A.** Left column, a positive control (AGL4-T4) exhibiting activation of *lacZ* (row1) and *HIS3* reporter genes (row2). Right column, a negative control (AGL4-T7 + an empty DB) lacking reporter activation. **B.** Rows 1 and 2, test for self-activation of reporter genes by 'prey' only; full FKD1 (column 1), the N-terminal (column 2), C-terminal (column 3), ARFA1e (column 4) and X102 (column 5). Rows 4 and 5, test for activation in the presence of 'preys' and an empty DB ('bait') vector. HIS3 assays assessed growth on histidine free media + 15mM 3AT at 28^{o}C after 4 days and X-gal assays incubated for 4 hours at 28^{o}C on 2 day old cells grown at 28^{o}C.

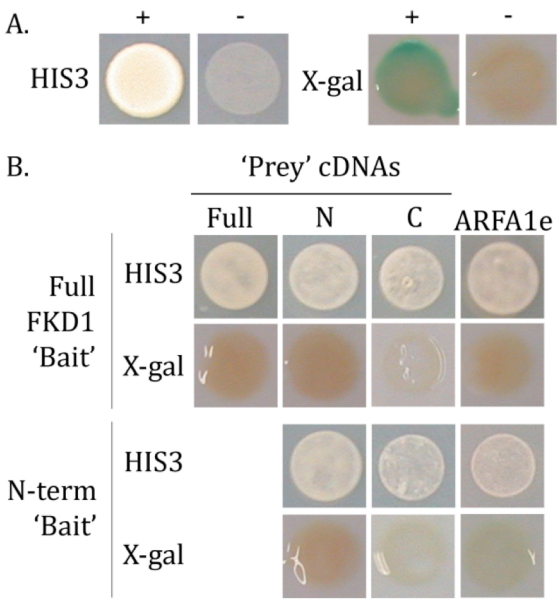

Figure 11. Assays to confirm protein-protein interaction between full FKD1 or N-terminal 'bait' constructs and Full FKD1, N-terminal, C-terminal, or ARFA1e 'preys'. **A.** Positive control (AGL4-T4) exhibiting activation of *HIS3* (column1) and *lacZ* reporter genes (column3). Negative control (AGL4-T7 + an empty DB) lacking *HIS3* activation (column2) or *lacZ* activation (column4). **B.** Rows 1 and 2, test for interactions with full FKD1 'bait' with full FKD1 (column 1), the N-terminal (column 2), C-terminal (column 3), and ARFA1e (column 4) 'preys'. Rows 3 and 4, test for activation in the presence of the N-terminal 'bait' construct. HIS3 assays assessed growth on histidine free media + 15mM 3AT at 28^{o}C after 4 days and X-gal assays incubated for 4 hours at 28^{o}C on 2 day old cells grown at 28^{o}C.

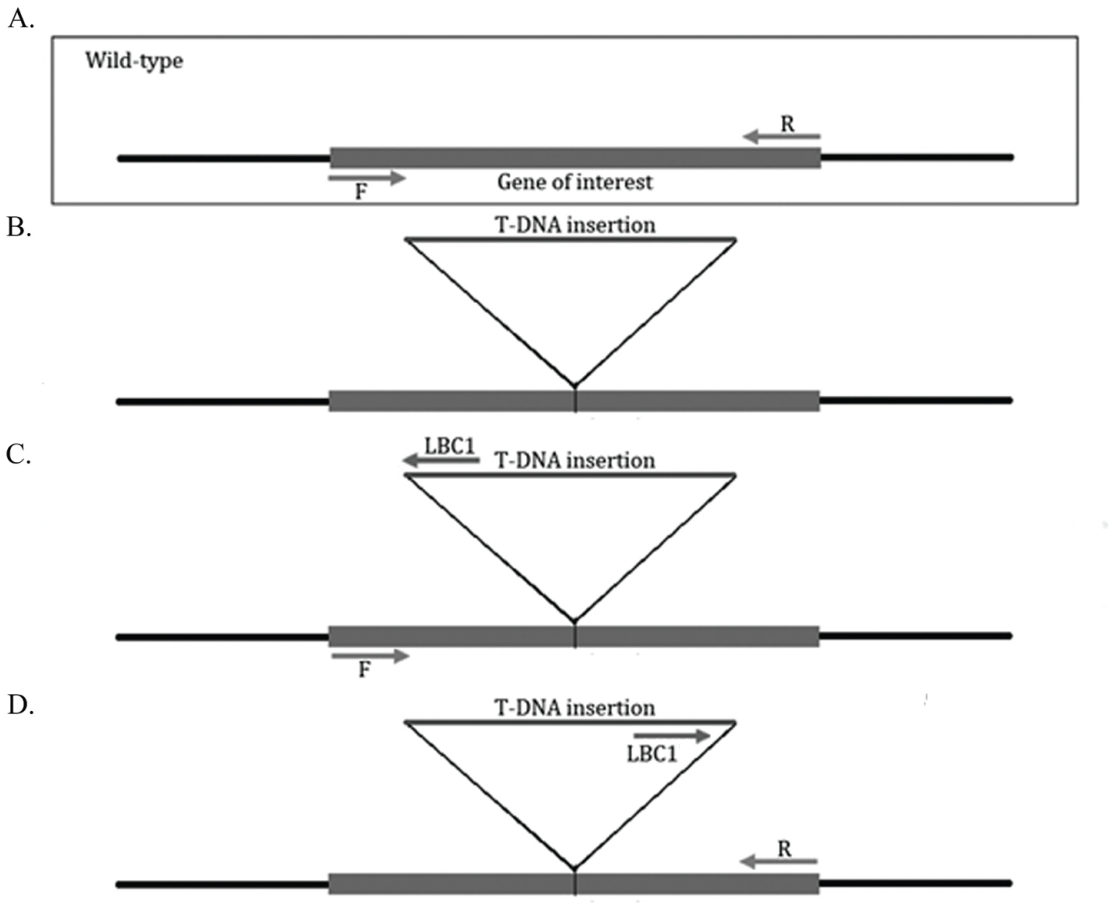

Figure 12. Schematic of PCR amplification utilized to identify plants harboring T-DNA insertion mutations in genes of interest. **A.** A PCR reaction using forward and reverse primers flanking the insertion site produces a product in the absence of a T-DNA insertion. **B.** An insertion separates the forward and reverse primers by a large distance, thus preventing amplification of the intervening sequence under our PCR conditions. In the presence of an insertion a PCR product is produced from a primer specific to the T-DNA insertion (LBC1) combined with either the forward primer (**C.**) or reverse primer (**D.**) flanking the insertion site.

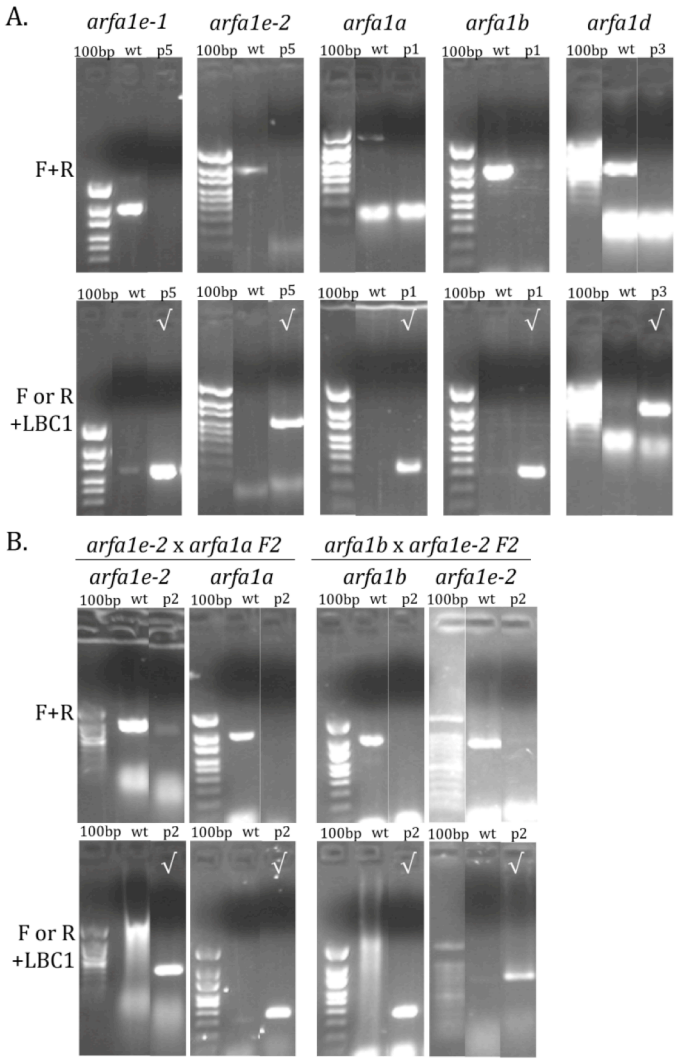

Figure 13. Gel figure showing PCR results used to identify plants homozygous for the T-DNA insertions associated with mutant alleles in members of the ARFA1 family. DNA isolated from individual plants (p1, 2, 3…) within populations segregating for the T-DNA insertion provided template for PCR reactions. Presence of the wild type allele was indicated by amplification using forward (F) and reverse (R) primers flanking the T-DNA insertion; presence of the insertion allele was indicated by amplification using F (or R) primer and a T-DNA specific primer LBC1. Samples were run next to a 100bp ladder, and a wild type control (wt) PCR reaction. **A.** Identification of plants homozygous for *arfa1e-1*, *arfa1e-2*, *arfa1a*, *arfa1b*, and *arfa1d* single mutations. In row 1, F and R primers were used; a PCR product indicates the wild type allele (seen only in wild type control). In row 2, F or R primer was used with LBC1 and PCR product (denoted by √) indicates the insertion allele. **B.** Identification of plants homozygous for *arfa1e-2 arfa1a*, and *arfa1b arfa1e-2* double mutants in an F2 population. Row 1 identifies the presence of a wild type allele (seen only in wild type control), and Row 2 an insertion allele. Double mutants are identified as plants with insertion alleles in both genes.

Appendix

Chemicals

3AT – 3-amino-1', 2', 4'-triazole (BioShop Canada Inc., Burlington, ON)

Bactotryptone (Bioshop Canada Inc., Burlington, ON)

β-mercaptoethanol (Sigma, St. Louis, MO, USA)

Chloroform (BDH Inc., West Chester, PA, USA)

Chloralhydrate (Pharmascience, Montreal, OC)

CTab (Sigma, St. Louis, MO, USA)

Cytoseal (Richard Allan Scientific, Houston, TX, USA)

D-glucose (Bio Basic Inc. Markham, ON)

EDTA (BDH Inc., West Chester, PA, USA)

Ethanol (EMD Chemicals Inc., Gibbstown, NJ, USA)

Glycerol (EMD Chemicals Inc., Gibbstown, NJ, USA)

HCl (EMD Chemicals Inc., Gibbstown, NJ, USA)

Isopropanol (EMD Chemicals Inc., Gibbstown, NJ, USA)

KCl (Fisher Scientific Company, Pittsburg, PA, USA)

LiAc – Lithium acetate dihydrate (BioShop Canada Inc., Burlington, ON)

$MgCl_2$ (J.T. Baker, Austin, TX, USA)

$MgSO_4$ (J.T. Baker, Austin, TX, USA)

$NaHSO_3$ (J.T. Baker, Austin, TX, USA)

NaCl (BDH Inc., West Chester, PA, USA)

Na-EDTA – (J.T. Baker, Austin, TX, USA)

Na_2HPO_4 (BDH Inc., West Chester, PA, USA)

NaH_2PO_4 (BDH Inc., West Chester, PA, USA)

Nitrogen base (BioShop Canada Inc., Burlington, ON)

PEG – Polyethylene glycol 3350 (BioShop Canada Inc., Burlington, ON)

Sarkosyl (Sigma, St. Louis, MO, USA)

Sorbitol (J.T. Baker, Austin, TX, USA)

Tris (EMD Chemicals Inc., Gibbstown, NJ, USA)

Tris-HCL (EMD Chemicals Inc., Gibbstown, NJ, USA)

Trizma (BDH Inc., West Chester, PA, USA)

X-gal (Gold Biotechnology, St. Louis, MO, USA)

Yeast extract (Bio Basic Inc. Markham, ON)

Recipes

DNA total extraction buffer – 1 volume DNA extraction buffer pH 7.5 via HCl (31.8g Sorbitol, 6g Trizma, 0.84g EDTA in 500mL water + 3.8mg/mL Na-bisulfite added right before use), 1 volume nucleic lysis buffer pH 7.5 via HCl (20mL 1M Tris, 20mL 0.25M EDTA, 40mL 5M NaCL, 2g CTab – topped to 100mL with water), 0.4 volume 5% Sarkosyl

Chloralhydrate Solution – 8 chloralhydrate: 2 glycerol: 1 water

LB media (1L) – 10g Bactotryptone, 5g Yeast extract, 5g NaCl, top with water to 1L and add 15g Bacteriograde agar

LiAc solution pH 7.5 (5mL) – 0.5mL 10x (1M) LiAc, 0.5mL 10x TE (0.1M Tris-HCl, 0.01M EDTA pH 8 with HCl), 4mL sterile water

PEG solution (5mL) – 4mL 50% PEG, 0.5mL 10x LiAC, 0.5mL 10x TE

SD media (1L) – 20g D-glucose anyhydrous , 6.7g nitrogen base, 1.5g drop-out powder

S.O.C. (1L) – 900mL distilled water, 20g bactotryptone, 5g yeast extract, 2mL NaCl (5M), 2.5mL KCl (1M), 10mL $MgCl_2$ (1M), 10$MgSO_4$ (1M), 20mL D-glucose (1M), fill to 1L, filter sterilize.

TE Buffer – 10mM Tris-HCL (pH 8.0), 1mM Na-EDTA (pH 8.0)

Z-buffer – 60mM Na_2HPO_4, 40mM NaH_2PO_4, 10mM KCl, 1mM $MgSO_4$, to be stored at 4^oC until use, then add 2.7uL β-mercaptoethanol/mL, and 1mg/mL X-gal